

Unclas  
00/13 11134

COVER SHEET FOR TECHNICAL MEMORANDUM

TITLE- Lunar Flying Unit Trajectory and  
Sortie Analysis

TM-68-1022-2

DATE- March 15, 1968

FILING CASE NO(S)- 620

AUTHOR(S)- J. W. Powers

FILING SUBJECT(S)-

(ASSIGNED BY AUTHOR(S)- Apollo Applications Program  
Lunar Surface Missions  
Mobility Devices  
Trajectory Equations

ABSTRACT

Current Apollo Applications Program studies for lunar surface missions are evaluating the use of a lunar flying unit, (LFU). This small astronaut-flown vehicle can extend lunar surface area exploration capability, allow terrain inaccessible by other mobility systems to be visited, and provide astronaut surface rescue capability from the Lunar Module landing site if two units are provided.

Trajectory models and computer programs for multi-stop impulsive, constant altitude-constant velocity, and semi-ballistic trajectories have been developed for the LFU. The effect of different flight variables has been included.

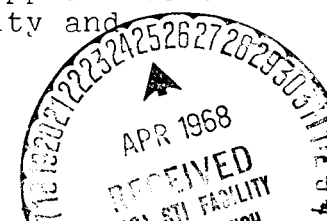
The derived non-impulsive trajectory equations are transcendental and lengthy. A simple algebraic approximate analysis has been developed which yields excellent agreement with the exact analysis for reasonable values of flight variables.

The capabilities of a baseline vehicle considered at the Summer Study of Lunar Science and Exploration, Santa Cruz, California, August 1967, are evaluated.

The baseline LFU optimum flight velocity and range for the constant velocity-constant altitude trajectory are relatively insensitive to small changes in altitude but decrease significantly with an increasing number of stops. For two and six stop trips the respective optimum velocities are 463 and 147 ft/sec. The corresponding maximum total ranges for two and six stops are 30.5 and 9.2 miles. When payload is carried both the optimum horizontal velocity and maximum total range further decrease with an increasing number of stops. With a 300 lb payload carried the total distance, the ranges for two and six stops are 14.9 and 4.3 miles respectively. The corresponding optimum velocities are 324 and 100 ft/sec.

The effect of system thrust/weight ratio on range is evaluated. A thrust/weight ratio of approximately 2:1 appears to be near the optimum relative to baseline LFU range capability and propulsion system throttling requirement.

SEE REVERSE SIDE FOR DISTRIBUTION LIST



# BELLCOMM, INC.

## LIST OF SYMBOLS

a	Range segment
A	Constant vertical acceleration
B	Payload loading stop, ( $B \leq N$ )
C	Propellant effective exhaust velocity
D	Vehicle thrust/weight ratio
g	Local lunar gravitational acceleration
h	Height increment
H	Total height
$I_{sp}$	Propellant specific impulse, ( $C/32.2$ )
K	Range proportionally constant, ( $R/a$ )
m	Propellant mass for trip segment
$\dot{m}$	Propellant mass flow rate
M	Mass
N	Number of stops
P	Payload mass
R	Range, total, (Statute Miles)
$\bar{R}$	Range, one way, (Statute Miles)
t	Time
V	Velocity
$\alpha$	Angle for optimum range
$\gamma$	Ratio, ( $\dot{m}/M$ )

## BELLCOMM, INC.

$\Delta V$	Velocity increment	
$\theta$	Descent angle	} Angles between thrust vector and horizontal lunar surface
$\phi$	Ascent angle	

### SUBSCRIPTS

A	Ascent phase
B	Payload loading stop
c	Coast phase
D	Descent phase
f	Final
H	Hover phase
M, MAX	Maximum
o	Initial
opt	Optimum
p	Propellant
V	Horizontal velocity
x	Horizontal Coordinate
y	Vertical Coordinate

# BELLCOMM. INC.

1100 Seventeenth Street, N.W. Washington, D. C. 20036

SUBJECT: Lunar Flying Unit Trajectory  
and Sortie Analysis  
Case 620

DATE: March 15, 1968

FROM: J. W. Powers

## TECHNICAL MEMORANDUM

### 1.0 INTRODUCTION

Current studies for the Apollo Applications Program Lunar Surface Missions are evaluating the use of lunar flying units (LFU) for surface mobility. Use of these small vehicles will significantly increase the lunar surface area exploration capability per mission as compared with foot mobility. The LFU also allows terrain inaccessible to other mobility systems to be traversed. Astronaut lunar surface rescue capability from the LM landing site by the other astronaut will be possible if two LFU's are provided per mission and if the rescue LFU payload capability is equal to a second suited astronaut's mass.

The purpose of this report is to perform an independent LFU trajectory study and to evaluate the range and payload characteristics of a LFU baseline configuration. Optimum and realistic trajectory bounds are considered.

### 2.0 LFU BASELINE CONFIGURATION

The baseline LFU configuration evaluated is one that was considered at the Summer Study of Lunar Science and Exploration held at Santa Cruz, California, July 31 to August 11, 1967. The characteristics of this vehicle in earth pounds mass are as follows:\*

Structural and Tank Weight,	150
Suited Astronaut Weight,	300
Maximum Propellant Weight,	230
Maximum Payload Weight,	300

Propulsion and attitude control are provided by two gimballed 125 lb thrust engines which can be differentially throttled down to 1/8th nominal thrust. LM descent stage

---

\*The current weight predictions are higher. These weight increases and performance implications are discussed in Section 7.0.

residual propellant can be used for the LFU. Based upon data from Reference (1), the specific impulses at the nominal and minimum thrust levels are 285 and 250 sec. The complex analysis and systems considerations relative to residual propellant use vs. loaded modular tanks, how much residual propellant will be available, extraction and refueling techniques will not be considered here.

The baseline vehicle is assumed to have the following capabilities: Rise, hover and descend over a given point; fly at near constant velocity and altitude; and take off and land at any desired attitude.

### 3.0 IMPULSIVE ANALYSIS

#### 3.1 Initial Considerations

Because of the near perfect vacuum above the lunar surface at altitudes of interest, the optimum LFU trajectory relative to propellant consumption is ballistic. To land at zero velocity, the launch impulsive velocity increment for a given range will have to be counteracted by an equal and opposite impulsive velocity increment applied at touchdown. Since both the range and maximum ordinate reached by this vehicle will be small compared with the lunar radius, the parabolic trajectory with no gravity acceleration variation with height is used. The moon's rotation will have negligible effect on the short ranges being considered and is ignored.

The actual minimum burn time of the baseline LFU configuration with both engines at maximum thrust is 262 sec., the unit is therefore far from approaching the impulsive optimum. Initial consideration of the simple impulsive optimum, however, fixes the upper performance boundary of any LFU configuration, allows qualitative comparisons to be made, and may permit the formulation of "rules of thumb" after the more complex realistic flight trajectories of Sections 5.0 and 6.0 are evaluated.

With elementary mechanics it is easily shown that the maximum horizontal range,  $R$ , of a projectile on a level surface in the absence of drag for a given impulsive velocity,  $V$ , in an area of local gravitational acceleration,  $g$ , is

$$R = \frac{V^2}{g} , \quad (1)$$

The launch velocity vector angle for maximum range is  $45^\circ$  relative to the horizontal. Return to the surface is with the launch velocity  $V$ .

If there is a difference in elevation,  $H$ , between the initial and final trajectory points, the maximum range for a given velocity increment without deceleration at landing is

$$R = 2 \sqrt{h (h \pm H)} \quad , \quad (2)$$

where  $h = \frac{V^2}{2g}$ . The optimum angle of projection,  $\alpha$ , for the trajectory with a difference in elevation between the launch and landing points is

$$\alpha = \tan^{-1} \sqrt{\frac{h}{h \pm H}} \quad , \quad (3)$$

The plus sign is used when the initial point is above the terminal point and the minus sign is used when the initial point is below the terminal point. Only trajectories which originate and terminate at the same elevation are further considered.

If the total impulsive velocity increment capability of a LFU is  $V$ , the maximum horizontal range with one stop and return to the point of projection with zero velocity is

$\bar{R} = \frac{1}{g} \left( \frac{V}{4} \right)^2$  \*. The available velocity increment must be equally apportioned to the beginning and end of both the out and return flight segments.

---

\* On linear paths a bar is used over the range symbol when a return trip is employed.  $\bar{R}$  is thus half the total distance traveled on any linear path. For one stop away from the origin,  $\bar{R} = R/4$ .

### 3.2 Impulsive Velocity and Multiple Stops

If there are  $N$  intermediate stops of distance  $a_i$  on a straight line path prior to return to the point of departure,

$$\sum_{i=1}^N a_i = R$$

The total velocity increment,  $\Delta V_i$ , for the distance  $a_i$  is  $\Delta V_i = 2\sqrt{a_i g}$ . Since  $a_i$  is proportional to  $R$ ,  $\Delta V_i = 2\sqrt{K_i \bar{R} g}$ . The velocity increment,  $\Delta V_{N+1}$ , for the return trip is

$2\sqrt{g \bar{R}}$ . Since the total velocity increment,  $V$ , is the sum of the individual increments, the range is

$$\bar{R} = \frac{V^2}{4g \left[ 1 + \sum_{i=1}^N \sqrt{K_i} \right]^2}, \quad (4)$$

If the distances  $a_i$  are equal,  $K = \frac{1}{N}$  and Equation (4) reduces to

$$\bar{R} = \frac{V^2}{4g(1 + \sqrt{N})^2}, \quad (5)$$

Equation (5) which yields the impulsive straight line range as a function of the number of stops for the base line LFU is shown in Figure I.

In the most probable multiple stop flight plan, the distances between the individual stops will not lie on a common straight line. With a polygonal path, the range will be greater than that indicated by Equations (4) and (5) since the distance back will always be less than the sum of the distances to the last stop.

For the polygonal path with  $N$  stops prior to return to the departure point, there will be  $(N + 1)$  segments of length  $K_1 R$ . For this case the total range is

$$R = \frac{V^2}{4 g \left[ \sum_{i=1}^{N+1} \sqrt{K_1} \right]^2}, \quad (6)$$

If the polygon sides are of equal length,  $K = \frac{1}{N+1}$  and Equation (6) reduces to

$$R = \frac{V^2}{4 g (N + 1)}, \quad (7)$$



It should be noted that the range given by Equations (6) and (7) is the total polygonal path traveled while that given by Equations (4) and (5) is half the linear distance traveled. Equation (7) is also shown in Figure I. For one stop prior to return, the polygonal path shows a total range of twice that of the linear path. This is of course the limiting case of a two sided polygon (straight line). The decreasing range of both the polygonal and linear path sorties **as** a function of an increasing number of stops is shown in Figure I.

### 3.3 Impulsive Velocity with Payload Carry Out or Return

This mode is evaluated in a manner similar to the previous example except for consideration of change in vehicle mass fraction at the time the payload is deposited or loaded. For a one stop trip, the total velocity increment for the trip out must equal the total velocity increment for the trip back. This requires that the vehicle mass fractions for the two trip segments be equal. The following quantities are defined:

Initial LFU mass,	$M_o$
Propellant mass,	$M_p$
Final mass,	$M_f = M_o - M_p$
Payload mass,	$P$
Propellant mass for trip out,	$m_1$ , (Payload from stop)
	$m_2$ , (Payload to stop)
Effective exhaust velocity,	$C$

If the payload is carried from the stop to the starting point, the vehicle mass fraction equality for the two trip segments is

$$\frac{M_o}{M_o - m_1} = \frac{M_o - m_1 + P}{M_f + P}$$

Solving for  $m_1$  using root with negative sign since  $m_1 < M_0$

$$m_1 = (M_0 + \frac{P}{2}) \left( 1 - \sqrt{1 - \frac{M_0 M_p}{(M_0 + \frac{P}{2})^2}} \right)$$

With this value of  $m_1$  the range is

$$\bar{R}_1 = \frac{\left[ c \ln \left( \frac{M_0}{M_0 - m_1} \right) \right]^2}{4 g}, \quad (8)$$

If the payload is carried from the initial point to the stop, the vehicle mass fraction equality for the two trip segments is

$$\frac{M_0 + P}{M_0 - m_2 + P} = \frac{M_0 - m_2}{M_f}$$

solving for  $m_2$  using root with negative sign since  $m_2 < M_0$

$$m_2 = M_0 + \frac{P}{2} - \sqrt{M_f (M_0 + P) + \frac{P^2}{4}}$$

with this value of  $m_2$  the range is

$$\bar{R}_2 = \frac{\left[ C \ln \left( \frac{M_O + P}{M_O - m_2 + P} \right) \right]^2}{4g}, \quad (9)$$

Equations (8) and (9) are shown in Figure II. For any given payload the range is greater when the payload is carried to the stop as compared with returning the same mass payload from the stop. As the payload mass increases, this range difference is seen to increase.

### 3.4 Impulsive Velocity with Multiple Stops and Payload Returned

If there are  $N$  equally-spaced stops on a straight line path with loading of the payload,  $P$ , at the  $B^{\text{th}}$  stop, the total velocity increments to the loading stop,  $\Delta V_1$ , and for the remaining trip segments,  $\Delta V_2$ , are

$$\Delta V_1 = 2B \sqrt{g \frac{R}{N}} = C \ln \left( \frac{M_O}{M_O - m_B} \right), \quad (10)$$

$$\Delta V_2 = 2(N - B) \sqrt{g \frac{R}{N}} + 2 \sqrt{g R} = C \ln \left( \frac{M_O - m_B + P}{M_f + P} \right)$$

where  $m_B$  is the propellant consumed in traveling to the  $B^{\text{th}}$  stop. Eliminating  $\frac{2}{C}\sqrt{gR}$  from the above equations yields an equation containing the propellant mass to the  $B^{\text{th}}$  stop in terms of trip constants.

$$\frac{M_O}{M_O - m_B} = \left[ \frac{M_O - m_B + P}{M_f + P} \right]^{\frac{B}{N - B + \sqrt{N}}}$$

The one way range may be determined by solving for  $m_B$  numerically and inserting in Equation (10). Figure III shows the baseline LFU straight line range as a function of both the payload and number of stops for payloads returned from the last stop prior to return ( $B = N$ ).

Consider  $N$  stops in a polygonal traverse with equal length segments and payload returned from the  $B^{\text{th}}$  stop. For a total traveled range,  $R$ , with  $N$  stops prior to return to the origin, the length of each segment will be  $(\frac{R}{N+1})$ . The total velocity increment required to the  $B^{\text{th}}$  stop is

$$\Delta V_i = 2B\sqrt{\frac{gR}{N+1}} = C \ln \left( \frac{M_O}{M_O - m_B} \right), \quad (11)$$

The velocity increment for the remaining legs of the traverse after the payload has been loaded is

$$\Delta V_2 = 2 (N - B + 1) \sqrt{\frac{g R}{N + 1}} = C \ln \left( \frac{M_O - m_B + P}{M_f + P} \right), \quad (12)$$

Where  $m_B$  is the propellant consumed in traveling the distance,  $(\frac{B}{N + 1}) R$ . Eliminating the quantity  $\frac{2}{C} \sqrt{\frac{g R}{N + 1}}$  from Equations (11) and (12) yields

$$\frac{M_O}{M_O - m_B} = \left( \frac{M_O - m_B + P}{M_f + P} \right)^{\frac{B}{N - B + 1}}, \quad (13)$$

Equation (13) can be solved numerically for  $m_B$  with assigned values of  $N$ ,  $B$  and  $P$ . With these values of  $m_B$  substituted in Equation (11), the total range for the baseline configuration may be determined as a function of the payload and number of intermediate stops. Figure IV shows the baseline LFU range for different values of  $N$  and  $P$  for the case of a payload returned from the last stop prior to return ( $B = N$ ). The baseline LFU range for the flight option of returning a payload from different loading stops is shown in Figure V.

4.0 HOVERING ANALYSIS

Section 3.0 considered the optimum LFU ballistic trajectory resulting from impulsive velocity increments. This section considers the more realistic problem of vertically rising above a point on the lunar surface to a fixed altitude, hovering for a time, and returning to the origin with zero velocity.\* Maximum hover time for any altitude will occur if maximum thrust is used in the ascent and decent phases to minimize the gravity loss.

This problem is analyzed by first considering zero hover altitude. The slight variation of specific impulse with thrust during the variable thrust hover phase is neglected in this analysis. At time,  $t$ , the LFU thrust,  $F$ , must equal the vehicle weight

$$F = (M_o - M_p) g$$

or

$$\dot{m}(t)C = (M_o - \int_0^t \dot{m}(t)dt) g$$

where  $\dot{m}(t)$  is the time varying propellant mass flow rate. With elementary dynamics\*\* the relationship between hover time,  $t_H$ , and propellant mass,  $M_p$ , for a hovering vehicle is

$$M_o - M_p = M_o \exp (-g t_H/C)$$

Solving for  $t_H$

$$t_H = -\frac{C}{g} \ln (1 - M_p/M_o) \quad , \quad (14)$$

---

\*If  $V$  is the velocity increment capability of a vehicle, the hover time at zero altitude is  $V/g$ .

\*\*By integration of  $Mg = -C dM/dt$

Figure VI shows maximum hover time as a function of vehicle propellant fraction,  $(\frac{M_p}{M_0})$ . It is interesting to note that for a given propellant specific impulse, there is no finite limit on the maximum hover time attainable if the vehicle propellant fraction approaches one. The hover time at zero altitude for the baseline LFU is 11.9 min. while the limiting hover time for a vehicle with a 0.9 propellant fraction is 66.3 min.

To determine the hover time at different altitudes above the lunar surface, the ascent phase is first considered.

The instantaneous acceleration,  $\ddot{y}$ , at any time of the powered ascent phase is

$$\ddot{y} = \frac{\dot{m}C}{M_0 - \dot{m}t} - g$$

The propellant mass flow rate,  $\dot{m}$ , is that constant value which yields maximum thrust. This  $\dot{m}$  will minimize the propellant expended to reach a specified altitude. Integrating  $\ddot{y}$  twice and inserting appropriate limits yields the altitude,  $h_A$ , attained during the powered portion of the ascent trajectory.

$$h_A = \frac{C M_0}{\dot{m}} \left[ \left(1 - \frac{\dot{m}}{M_0} t_A\right) \ln \left(1 - \frac{\dot{m}}{M_0} t_A\right) + \frac{\dot{m}}{M_0} t_A \right] - \frac{g t_A^2}{2}, \quad (15)$$

At the altitude,  $h_A$ , the LFU will have a velocity,  $V_A$ .

$$V_A = C \ln \left( \frac{M_0}{M_0 - \dot{m} t_A} \right) - g t_A$$

If the engines are shut down at the altitude  $h_A$ , the vehicle will coast to an additional height increment  $h_c$  where all the kinetic energy has been converted into potential energy. The total height,  $H$ , attained by thrusting for time  $t_A$  is

$$H = h_A + h_c$$

where

$$h_c = \frac{V_A^2}{2g}$$

After algebraic simplification

$$H = \frac{C}{\gamma_A} \ln (1 - \gamma_A t_A) + \frac{C^2}{2g} \left[ \ln (1 - \gamma_A t_A) \right]^2 + C t_A, \quad (16)$$

where

$$\gamma_A = \frac{\dot{m}}{M_O}$$

Equation (16) in different format is shown in Reference (2).

The hover time,  $t_H$ , is determined from Equation (14) considering the propellant apportionment for the three powered phases

$$t_H = -\frac{C}{g} \ln \left\{ 1 - \left[ \frac{M_p - \dot{m} (t_A + t_D)}{M_O - \dot{m} t_A} \right] \right\}, \quad (17)$$



Equation (17) relates the total propellant division during the three powering phases, ascent, hover and descent. Retro velocity is provided by engine operation at full thrust for the descent time,  $t_D$ . With free fall for a distance,  $h_D$ ,

from the hover altitude,  $H$ , prior to engine ignition, a velocity  $\sqrt{2g h_D}$  is acquired. A zero velocity landing with engine ignition at an altitude  $H - h_D$  above the lunar surface requires a retro velocity

$$\sqrt{2g h_D} + g t_D = C \ln \left( \frac{M_f + \dot{m} t_D}{M_f} \right), \quad (18.1)$$

The distance traveled during the powered descent phase\* with ignition at an altitude  $H - h_D$  is

$$H - h_D + \frac{C}{\gamma_D} \left[ (1 - \gamma_D t_D) \ln (1 - \gamma_D t_D) + \gamma_D t_D \right] = \sqrt{2g h_D} t_D + \frac{g t_D^2}{2}, \quad (18.2)$$

$\gamma_D$  is defined on Page 16

Equations (16), (17), (18.1) and (18.2) are solved numerically for hover time as a function of hover altitude. This relationship for the baseline LFU is shown in Figure VII and exhibits the decreasing hover time with increasing altitude.

## 5.0 CONSTANT ALTITUDE AND CONSTANT HORIZONTAL VELOCITY TRAJECTORY

With the impulsive trajectory, the resultant range segment is determined by the magnitude and inclination of the applied velocity increment. In a constant velocity-constant altitude trajectory, the LFU thrust is maintained equal to the instantaneous lunar vehicle weight after a desired horizontal velocity and attitude are attained. This trapezoidal shaped trajectory allows the selection of any landing point along the line of flight without  $\Delta V$  loss if the point is observed in time to retro. The constant altitude-constant velocity trajectory is a variant of the hovering analysis developed in Section 4.0. During the ascent phase, the LFU rises at full thrust and constant attitude,  $\phi$ , with respect to the lunar surface.\*\* At an altitude where the desired horizontal

---

\* If  $\dot{m} t_A$  is small compared with  $M_0$ ,  $t_D \approx t_A M_f / M_0$ .

\*\* Actual flight profiles will most probably include short segments of vertical flight at the start and finish of each trajectory element.

velocity component,  $V_x$ , is reached the engines are shut down\* and the vertical velocity component causes the vehicle to coast to the operating altitude,  $H$ . Horizontal flight is at constant altitude with the thrust maintained equal to the exponentially decreasing weight. Descent is accomplished at a constant attitude,  $\theta$ , with both the horizontal and vertical velocity components being reduced to zero at landing. An unpowered coast phase is used between the end of the hover phase and start of powered descent.

The altitude,  $H$ , is reached with the engines operating at maximum thrust at a constant angle,  $\phi$ , to the horizon for the time,  $t_A$ . To determine the altitude  $H$  as a function of the ascent time,  $t_A$ , and attitude,  $\phi$ , the characteristic velocity,  $C$ , in Equation (16) is replaced by  $C \sin \phi$ .

$$H = \frac{C \sin \phi}{\gamma_A} \ln (1 - \gamma_A t_A) + \frac{(C \sin \phi)^2}{2g} \left[ \ln (1 - \gamma_A t_A) \right]^2 + C \sin \phi t_A, \quad (19)$$

Figure VIII shows the constant velocity-constant altitude trajectory model.

The horizontal velocity component,  $V_x$ , can be written in terms of the ascent and descent phase mass fractions, attitude angles, and times. The powered portion of the descent phase is conducted at maximum thrust.

$$V_x = C \cos \phi \ln \left( \frac{M_O}{M_O - \dot{m} t_A} \right) = C \cos \theta \ln \left( \frac{M_f + \dot{m} t_D}{M_f} \right), \quad (20)$$

---

\*In practice the LFU engines would not be shut down during any flight but would be throttled down to minimum thrust which is approximately one-eighth the nominal value. Although this refinement with its attendant complexity could be introduced into the analysis, assuming zero thrust for the coast phases will not introduce significant error in the results.

Equation (20) requires that the sum of the horizontal velocity components be zero at landing. During the powered descent phase the sum of positive and negative displacements is zero

$$H - \frac{g t_{cD}^2}{2} + \frac{C \sin \theta}{\gamma_D} \left[ (1 - \gamma_D t_D) \ln(1 - \gamma_D t_D) + \gamma_D t_D \right] - \frac{g t_D^2}{2} - g t_{cD} t_D = 0, \quad (21)$$

At the end of the hover phase the LFU free falls for a time,  $t_{cD}$ , prior to initiation of constant attitude-constant thrust powered descent. At the instant of landing the sum of the vertical velocity components is zero

$$0 = -g(t_{cD} + t_D) + C \sin \theta \ln \left( \frac{M_f + \dot{m} t_D}{M_f} \right), \quad (21.1)$$

The horizontal range,  $R$ , consists of three segments,  $R_\phi$ ,  $R_V$ , and  $R_\theta$ .  $R_\phi$  and  $R_\theta$  are the horizontal projections of the powered portions of the ascent phase and descent phase trajectories.

$$R_\phi = \frac{C \cos \phi}{\gamma_A} \left[ (1 - \gamma_A t_A) \ln(1 - \gamma_A t_A) + \gamma_A t_A \right], \quad (22)$$

$$R_\theta = \frac{C \cos \theta}{\gamma_D} \left[ (1 - \gamma_D t_D) \ln(1 - \gamma_D t_D) + \gamma_D t_D \right], \quad (23)$$

where

$$\gamma_D = \frac{\dot{m}}{M_f + \dot{m} t_D}$$

The center range segment,  $R_V$ , is flown at the constant horizontal velocity,  $V_x$ , and includes the hover time plus the ascent and descent coast times. Ascent coast time,  $t_{cA}$ , is the time from the end of the powered ascent phase to arrival at altitude,  $H$ , with zero vertical velocity.\*

$$t_{cA} = \frac{C}{g} \sin \phi \ln \left( \frac{M_O}{M_O - \dot{m} t_A} \right) - t_A, \quad (24)$$

The range segment,  $R_V$ , is the product of the constant horizontal velocity,  $V_x$ , and the sum of the coast and hover times. Using Equations (17) and (24) yields the constant velocity range segment. Descent coast time may be eliminated from (25) and (26) with (21.1).

$$R_V = \frac{V_x C}{g} \left\{ \sin \phi \ln \left( \frac{M_O}{M_O - \dot{m} t_A} \right) - \ln \left( 1 - \left[ \frac{M_P - \dot{m} (t_A + t_D)}{M_O - \dot{m} t_A} \right] \right) - \frac{g}{C} (t_A - t_{cD}) \right\} \quad (25)$$

By adding Equations (22), (23) and (25) and eliminating  $\cos \theta$  from Equation (23) by use of Equation (20), the total one stop range,  $R$ , is

$$R = \frac{C \cos \phi}{\gamma_A} \left[ (1 - \gamma_A t_A) \ln (1 - \gamma_A t_A) + \gamma_A t_A \right] +$$

---

\* Total flight time is  $(t_A + t_{cA} + t_H + t_{cD} + t_D)$

$$\begin{aligned}
& + \frac{V_x C}{g} \left\{ -\ln \left( 1 - \frac{\frac{M_p}{M_o} - \gamma_A (t_A + t_D)}{1 - \gamma_A t_A} \right) - \sin \phi \ln (1 - \gamma_A t_A) - \frac{g}{C} (t_A - t_{cD}) \right\} \\
& + \left( \frac{V_x}{\gamma_D} \right) \left\{ \frac{1}{\ln \left( \frac{M_f + m t_D}{M_f} \right)} \right\} \left[ (1 - \gamma_D t_D) \ln (1 - \gamma_D t_D) + \gamma_D t_D \right], \quad (26)
\end{aligned}$$

To determine the LFU range with return capability, Equation (26) must be equal for both the out and return trip segments for a given total propellant mass. If the range equations for the out segment,  $R_1$ , and return segment,  $R_2$ , are written symbolically in terms of the initial mass,  $M_o$ , and propellant mass,  $M_p$ , the solution may be indicated for an iterative computation

$$\bar{R}_1 = R(M_{o1}, M_{p1}, \dots)$$

$$\bar{R}_2 = R(M_{o2}, M_{p2}, \dots) = \bar{R}_1$$

subject to the following conditions:

$$M_{o1} = M_o$$

$$M_{o2} = M_o - M_{p1}^*$$

$$M_p = M_{p1} + M_{p2}$$

---

\* If a payload mass is returned, it must be included in  $M_{o2}$

The launch angle,  $\phi$ , and the horizontal flight velocity,  $V_x$ , are not independent of the LFU characteristics since the vertical thrust component must exceed the vehicle lunar weight if any altitude is to be attained. For zero operational altitude, the flight attitude angle is

$$\sin \phi_{\min} = (M_0 - \dot{m}t) g / (\dot{m}C)$$

At zero time this angle is  $26.7^\circ$  for the baseline LFU. If this decreasing angle is maintained at its minimum value until a required horizontal velocity is developed, the vehicle will not rise above the lunar surface and minimum acceleration time occurs. The nonuniform lunar surface and visibility considerations require a trajectory with finite altitude. With increasing launch angles a longer time is required to develop a given horizontal velocity and the altitude attained increases correspondingly. This type of trajectory could incorporate a turn rate,  $\dot{\phi} = \dot{\phi}(t)$ , for the transition to and from the hover phase. A variable thrust profile could also be utilized to eliminate both the coast ascent and coast descent phases.

For a given vehicle, an upper limit exists on the launch angle to attain a given horizontal velocity component. At this limit the trajectory shape is triangular since the time of flight at constant altitude will be zero. This shape is a consequence of consuming all the propellant in the ascent and descent phases. With maximum ascent angle and a given horizontal velocity, the range will be minimum and the altitude a maximum. A representation of the minimum and intermediate range trajectories is shown in Figure VIII.

Figure IX shows the relationship between trajectory height and ascent angle for different flight velocities. The relationship between range and ascent angle for different flight velocities is shown in Figure X. The insensitivity of range variation with increasing ascent angles for low flight velocities is apparent. The total flight times for different flight velocities as a function of ascent angle is shown in Figure XI. The decreasing flight time with increasing horizontal velocity for a given ascent angle is caused by the vehicle having to operate at full thrust for longer ascent and descent phases. As the flight velocity is reduced to zero, the total flight time approaches the hover time at zero altitude (11.9 min for the baseline LFU, see Section 4.0).

For the constant altitude-constant velocity trajectory, the optimum velocity for a given vehicle at a specified altitude is of interest. Figure XII shows the range as a function of the horizontal velocity for different ascent angles (altitudes).

The range for a given horizontal velocity is a maximum at an ascent angle of approximately  $60^\circ$  for the baseline vehicle. For each ascent launch angle there is an optimum flight altitude which maximizes the vehicle range. With increasing horizontal velocity, the optimum altitude is seen to increase (Figure XII). Multiple stop trajectories which require both high horizontal velocities and high altitudes (ascent angles) may not be possible for a given vehicle. This is a consequence of using too much of the available propellant in the initial take-off and landing phases. For the baseline LFU, two-stop trajectories with an ascent angle of  $70^\circ$  and a horizontal velocity of 1000 ft/sec are possible.

The numerical calculations show that the baseline LFU propellant consumption for the out and return trip segments of a given constant velocity-constant attitude angle flight is independent of the trajectory height and horizontal velocity. For velocities of 100 to 500 ft/sec and altitudes of 50 to 22,500 ft, the propellant required for the out and return trip segments is constant at approximately 127 and 103 lbs. If the baseline LFU flies an impulsive trajectory, the propellant consumed for the out and return trip segments is identical to that expended in the "real" trajectories.

If a two segment profile is flown at constant horizontal velocity and launch angle, with return to the point of departure, different altitudes will result for the out and return trip segments. This is a consequence of constant force acceleration of the lighter vehicle during the return trip ascent segment. The vehicle thus achieves the required horizontal velocity in shorter time and the vertical velocity component and altitude at the end of powered ascent will be correspondingly greater. The higher vertical velocity component thus yields a greater coast height increment. To maintain constant altitude for the out and return trip segments with the proposed trajectory model requires that the return trip ascent angle be decreased.

At constant launch angle the maximum total range and optimum horizontal velocity of a two stop trip are both significantly reduced as compared with a one stop trip. This is a consequence of the two stop flight optimizing at a much lower altitude and corresponding horizontal velocity. At constant horizontal velocity the total range is reduced by introducing the additional stop as a result of the intrinsic energy loss. The corresponding baseline total range reductions for two-stop sorties as compared with one stop sorties are 4.3% and 9.1% for horizontal velocities of 100 and 200 ft/sec at an ascent angle of  $30^\circ$ .

### 5.1 Constant Altitude and Constant Horizontal Velocity Trajectory, Approximate Analysis

In Section 5.0 a lengthy transcendental range Equation, (26), was developed for the constant altitude and constant velocity trajectory. Solution of this equation requires repeated iterative calculations and increasing the number of stops greatly increases computational difficulty. Using several simplifying assumptions and a rectangular rather than trapezoidal profile permits development of a simple algebraic range function which yields satisfactory accuracy for initial evaluation purposes. The assumptions are as follows:

- The vehicle maintains a constant vertical ascent and descent acceleration for all trajectory segments.
- At the end of the powered ascent phase, the vertical thrust vector is rotated  $90^\circ$  and the horizontal velocity component develops during the vertical coast phase. This results in the vehicle arriving at the operational altitude with zero vertical velocity and the desired horizontal velocity.
- At the beginning of the constant altitude phase, the thrust vector is rotated to the original position and the thrust is maintained equal to the lunar vehicle weight.
- The descent phase is the reverse of the ascent phase.

If  $D$  is the initial vehicle lunar thrust to weight ratio, the ascent acceleration,  $A$ , is

$$A = (D-1)g$$

The operating altitude,  $H$ , consists of the height attained during the powered ascent,  $h_A$ , plus the coast height increment,  $h_c$ .

$$H = h_A + h_c = \frac{1}{2} A t_A^2 + \frac{1}{2g} (A t_A)^2$$

Solving for the ascent time,  $t_A$ , as a function of the vehicle thrust to weight ratio

$$t_A = \sqrt{\frac{2H}{g(D-1)D}}$$



If  $\Delta V$  is the total vehicle velocity increment, the velocity distribution for  $N$  stops is

$$\Delta V = 2 N V_x + 2 N g D t_A + g t_V$$

where  $t_V$  is the flight time at the constant horizontal velocity  $V_x$ . If  $R_V$  is the range segment flown at constant velocity,  $t_V = R_V/V_x$ . Solving for the range segment  $R_V$

$$R_V = \frac{V_x}{g} \left[ \Delta V - 2N \left( \sqrt{\frac{2gD}{(D-1)}} + V_x \right) \right]$$

The relationship between ascent time,  $t_A$ , and coast time,  $t_c$ , is

$$t_c = \frac{A t_A}{g} = (D-1) t_A$$

Since the horizontal velocity component  $V_x$  is assumed to develop during the coast time

$$V_x = A_x t_c = A_x (D-1) t_A$$

where  $A_x$  is the constant horizontal acceleration, ( $A \neq A_x$ ).

The horizontal distance,  $R_x$ , traveled by the vehicle in developing the horizontal velocity component is

$$R_x = \frac{V_x}{2} (D-1) t_A$$

The total range,  $R$ , for  $N$  stops is

$$R = R_v + 2 N R_x$$

After introducing the previously developed terms

$$R = \frac{V_x}{g} \left\{ \Delta V - N \left[ (D+1) \sqrt{\frac{2gH}{(D-1)D}} + 2 V_x \right] \right\}, \quad (27)$$

For a given vehicle ( $\Delta V$  and  $D$  constant) and a specified operational altitude,  $H$ , the optimum horizontal velocity for maximum range is

$$\left( V_x \right)_{\text{opt}} = \frac{\Delta V - N(D+1) \sqrt{\frac{2gH}{(D-1)D}}}{4 N}, \quad (28)$$

By using Equation (28) in Equation (27), the maximum range of a given vehicle is

$$R_{\text{MAX}} = \frac{1}{8 Ng} \left[ \Delta V - N (D+1) \sqrt{\frac{2g H}{(D-1)D}} \right]^2, \quad (29)$$

Probable flight altitudes will be low compared with the vehicle total velocity increment capability. For low\* vehicle thrust to weight ratios and a small number of stops, Equation (29) may be written to a good approximation as

$$R_{\text{MAX}} = \frac{\Delta V^2}{8 Ng}$$

A N stop impulsive vehicle of total velocity increment capability  $\Delta V$  will have a maximum range

$$R_{\text{MAX}} = \frac{\Delta V^2}{4 Ng}$$

The ratio of maximum range for the optimum impulsive flight to maximum range for the optimum constant altitude-constant velocity flight is therefore 2:1. This surprisingly simple approximate result can be used as a "rule of thumb" with the impulsive results developed in Section 3.0. An approximate many stop range equation is developed in Appendix I.

---

\*1.5 < D < 2.5

For impulsive velocity trajectories, the relationship between range, R, and specific impulse,  $I_{sp}$ , is

$$\frac{R_1}{R_2} = \left( \frac{I_{sp1}}{I_{sp2}} \right)^2$$

This simple ratio may also be applied to the constant velocity-constant altitude trajectory with good accuracy if the flight velocities, flight altitudes and number of stops are small compared with the vehicle velocity increment.

The accuracy of approximate Equation (27) compared with "exact" Equation (26) is shown in the following Table.

Horizontal Velocity ft/sec	Flight Altitude ft	Range % Error	
		1 Stop	2 Stops
100	60	-2.2	- 5.0
300	559	-4.5	-11.7
500	1605	-7.4	-22.0

The flight altitudes are those resulting from a constant 30° attitude ascent trajectory. In flight profiles where significant error is encountered (>500 ft/sec and >2 stops), the results will be conservative.

The baseline LFU total range as a function of the number of stops and horizontal velocity for a 50 ft trajectory altitude is shown in Figure XIII. The range advantage of flight at low horizontal velocity for a many-stop profile is apparent. Figure XIV shows the baseline LFU maximum total range, Equation (29), as a function of number of stops for different payloads and a 50 ft altitude. The decreasing optimum horizontal velocity at a 50 ft altitude as a function of both an increasing number of stops and an increasing payload is shown in Figure XV.

Increasing the trajectory height while keeping other flight variables constant will decrease the range since an energy expenditure is required for the potential energy increase and decrease of each trajectory segment. The percentage range decrease with altitude is greater for increasing horizontal velocities and an increasing number of stops as shown in Figure XVI.

If many-stop LFU flight profiles are used, the vehicle will optimize at low altitude and flight velocity. These conditions will, of course, minimize astronaut injury probability in event of an inflight malfunction.

## 5.2 Effect of Propulsion System Thrust/Weight Ratio on LFU Range

Improper selection of the propulsion system thrust/weight (F/W) ratio will reduce vehicle range. High F/W ratios will also significantly affect rocket engine characteristics since the throttling requirement for a given vehicle will increase as a function of the F/W ratio. With high engine throttability requirements ( $>8:1$ ), rocket engine design, development, and performance problems can be anticipated.

Examination of the factor  $(D+1)/\sqrt{(D-1)D}$ , where D is the vehicle F/W ratio, in range Equations (27) and (29) reveals a range increase with increasing F/W ratios. The limiting value of the factor with an infinite (impulsive) F/W ratio is one.

The baseline vehicle's initial F/W ratio with no payload is 2.23. By increasing the vehicle's F/W ratio over some arbitrary minimum (1.1), the attainable range will increase. Figure XVII shows the percentage range increase as a function of different horizontal velocities and number of stops for a 100 ft altitude. Percent range change is seen to be relatively insensitive to horizontal velocity change at a given F/W ratio for one stop, with maximum increase occurring at maximum velocity. Both the range increase and velocity sensitivity are seen to significantly increase with an increasing number of stops. The "knee" of this family of curves occurs at a F/W ratio of approximately two.

Considerations of single engine operation in a multi-engine system vs. pure dual engine operation will not be discussed here. It should be noted, however, that if a dual engine system is required to be capable of single engine operation, the propulsion system is significantly penalized. A dual engine system with single engine operational capability requires a 100% throttability increase as compared with normal two-engine operation. The integrated average specific impulse of a high throttle range engine will be significantly reduced if a large percentage of the propellant is consumed at the low thrust level.

## 6.0 SEMI-BALLISTIC TRAJECTORY

Section 3.0 considered the optimum ballistic trajectory with impulsive velocity increments at the initial and terminal trajectory points. This section will consider the ballistic trajectory with finite acceleration and deceleration times. During the coast phase the engines are throttled down to minimum thrust and the thrust vector is directed upward. The coast phase may be considered as ballistic with a time decreasing lunar gravity acceleration resulting from the low vertical constant thrust acting on the vehicle of constantly decreasing mass.\* This type of trajectory will require a guidance and control system so that the appropriate initial velocity magnitude and direction for a desired range can be determined. Only trajectory elements will be considered here.

The equations developed in Section 5.0 for ascent and descent at maximum thrust and constant attitude are used for the initial and final trajectory elements. After an ascent burn time,  $t_A$ , at constant attitude,  $\phi$ , the LFU will rise to an altitude,  $h_A$ , which is equal to the  $h_A$  of Equation (15) with  $C \sin \phi$  substituted for  $C$ . At this point the LFU has horizontal and vertical velocity components  $V_{Ax}$  and  $V_{Ay}$ .

$$V_{Ax} = V_A \cos \phi$$

$$V_{Ay} = V_A \sin \phi - g t_A$$

$$V_A = -C \ln (1 - \gamma_A t_A)$$

During the coast phase time,  $t_c$ , the throttled engines are thrusting upward with an effective exhaust velocity,  $C_c$ , ( $C > C_c$ ). The LFU altitude  $h_c$ , at the end of the coast phase just prior to initiation of the descent phase is

$$h_c = h_A + V_{Ay} t_c + \frac{C_c}{\gamma_c} \left[ (1 - \gamma_c t_c) \ln (1 - \gamma_c t_c) + \gamma_c t_c \right] - \frac{g t_c^2}{2}, (30)$$

---

\*Figure XVIII shows the trajectory model.

where

$$\gamma_c = \frac{\dot{m}_c}{M_0 - \dot{m} t_A}, \quad (\dot{m} > \dot{m}_c)$$

At the end of the semi-ballistic coast phase, the LFU velocity components at the altitude  $h_c$  are

$$V_{cx} = V_{Ax}$$

$$V_{cy} = V_{Ay} + V_c - g t_c$$

$$V_c = -C_c \ln (1 - \gamma_c t_c)$$

To land with zero velocity at the end of the descent phase, the required horizontal,  $V_{Dx}$ , and vertical,  $V_{Dy}$ , retro velocity components are

$$V_{Ax} = V_{Dx} = V_D \cos \theta, \quad (31.1)$$

$$V_{cy} + V_{Dy} = 0, \quad (31.2)$$

where

$$V_D = C \ln \left( \frac{M_f + \dot{m} t_D}{M_f} \right)$$

$$V_{Dy} = V_D \sin \theta - g t_D$$

Prior to initiation of descent thrust, the vehicle is at an altitude,  $h_c$ , with a vertical velocity component  $V_{cy}$ . During the descent phase, the sum of positive and negative displacements is zero.

$$h_c + \frac{C \sin \theta}{\gamma_D} \left[ (1 - \gamma_D t_D) \ln (1 - \gamma_D t_D) + \gamma_D t_D \right] - \frac{g t_D^2}{2} + V_{cy} t_D = 0 \quad (32)$$

The total horizontal range,  $R$ , consists of three segments, the ascent segment,  $R_\phi$ , the coast segment,  $R_V$ , and the descent segment,  $R_\theta$ .  $R_\phi$  and  $R_\theta$  are equal to Equations (22) and (23). The coast segment,  $R_V$ , is the product of the horizontal velocity component,  $V_{Ax}$ , acquired at the end of the ascent phase and the coast time,  $t_c$ .

$$R_V = -C \cos \phi \ln (1 - \gamma_A t_A) t_c, \quad (33)$$

The total flight time is  $t_A + t_c + t_D$  and the total mass of propellant in terms of the respective times and mass flow rates is

$$M_p = \dot{m} (t_A + t_D) + \dot{m}_c t_c, \quad (34)$$



The horizontal range,  $R$ , is the sum of Equations (22), (33) and (23).

$$\begin{aligned}
 R = & \frac{C \cos \phi}{\gamma_A} \left[ (1 - \gamma_A t_A) \ln (1 - \gamma_A t_A) + \gamma_A t_A \right] \\
 & - C \cos \phi \ln (1 - \gamma_A t_A) t_c \\
 & + \frac{C \cos \theta}{\gamma_D} \left[ (1 - \gamma_D t_D) \ln (1 - \gamma_D t_D) + \gamma_D t_D \right], \quad (35)
 \end{aligned}$$

The basic unknowns in this trajectory for a given vehicle are the three time increments, constant ascent and descent angles, altitude at the end of the coast phase, and range. During ascent, either the ascent time,  $t_A$ , or the ascent angle,  $\phi$ , is fixed. Numerical solution of Equations (30), (31.1), (31.2), (32), (34), and (35) yields the desired horizontal range.

The maximum trajectory ordinate,  $h_M$ , for a given semi-ballistic flight may be of interest. At the maximum ordinate, the vertical velocity component is zero. If  $t_M$  is the time measured from the end of the ascent trajectory phase, the sum of positive and negative vertical velocity components at the maximum ordinate is

$$0 = V_A \sin \phi - g t_A + C_c \ln \left[ \frac{M_O - \dot{m} t_A}{M_O - \dot{m} t_A - \dot{m}_c t_M} \right] - g t_M, \quad (36)$$

Equation (36) is solved numerically for  $t_M$ . The maximum ordinate is calculated from Equation (30) with the substitution of  $t_M$  for  $t_c$ .

A constraint noted for the constant altitude-constant velocity trajectory in Section 5.0 was that the vertical thrust component must exceed the instantaneous lunar weight during ascent. This constraint is also valid for the semi-ballistic trajectory since the powered ascent phases of both trajectories are identical.

With the constant velocity-constant altitude trajectory of Section 5.0, specification of both ascent angle ( $\phi$ ) and ascent burn time ( $t_A$ ) is required to establish the flight altitude and horizontal velocity. Specification of either  $\phi$  or  $t_A$  for the semi-ballistic trajectory fixes the profile for a required range. With the proposed model, descent times ( $t_D$ ) and angles ( $\theta$ ) are less than corresponding ascent times and angles. The ratio of  $t_D/t_A$  for maximum range is 0.857 for both segments of a baseline LFU round trip.  $\theta$  is between  $1^\circ$ - $3^\circ$  less than  $\phi$  ( $30^\circ \leq \phi \leq 70^\circ$ ) for a two segment sortie.

Figure XIX shows the effect of ascent angle on LFU one way range. The maximum range of 21.8 miles occurs at an ascent angle of approximately  $45^\circ$ . Baseline vehicle maximum semi-ballistic range occurs at nearly exactly the same ascent angle ( $45^\circ$ ) as does the maximum impulsive range. The semi-ballistic baseline LFU's round trip range is 68% of that attainable by an impulsive theoretical vehicle.

Trajectory maximum altitude as a function of ascent angle is also shown in Figure XIX. The maximum altitude at the maximum range condition is 17,900 ft. for the return trip segment. Maximum trajectory altitude for an impulsive vehicle is 25% of the maximum range. The corresponding altitude for the baseline LFU semi-ballistic trajectory is 14% of the maximum range. The corresponding horizontal velocity for a round trip maximum range sortie is 600 ft/sec.

The maximum traveled distance for a one segment trip is 87.2 miles while the total traveled distance for an optimum two segment trip is 43.6 miles. This 50% total range reduction shows the great sensitivity of the semi-ballistic trajectory range with an increasing number of stops. This sensitivity is much greater than that experienced in a multiple stop constant velocity-constant altitude trajectory flight of moderate altitude and velocity. Maximum range for the baseline LFU optimum semi-ballistic trajectory is 88% of the optimum constant velocity-constant altitude trajectory range for a single stop round trip.

### 6.1 SEMI-BALLISTIC TRAJECTORY, APPROXIMATE ANALYSIS

Significant simplification is introduced in the semi-ballistic trajectory analysis if the descent phase is assumed symmetrical to the ascent phase. This assumption requires  $\phi = 0$ ,  $t_A = t_D$ , and  $h_A = h_c$ . Conservative range will result with this trajectory model since for an efficient descent profile  $t_D < t_A$ . With the proposed assumption the coast phase, flown at a constant horizontal velocity, is reduced and the total range is correspondingly decreased.

The total propellant mass in terms of times and propellant mass flow rates is

$$M_p = 2 \dot{m} t_A + \dot{m}_c t_c, \quad (37)$$

Descent phase initiation occurs after the vehicle has descended to the ascent phase altitude after a coast phase time,  $t_c$ . The summation of vertical displacements occurring during the coast phase is

$$V_{Ay} t_c + \frac{C}{\gamma_c} \left[ (1 - \gamma_c t_c) \ln (1 - \gamma_c t_c) + \gamma_c t_c \right] - \frac{g t_c^2}{2} = 0, \quad (38)$$

Equation (38) is (30) with  $h_c - h_A = 0$ . Total range is

$$R = 2 R_\phi + R_v, \quad (39)$$

where  $R_\phi$  and  $R_v$  are defined by Equations (22) and (33).

The approximate maximum range determined by numerical solution of Equations (37), (38), and (39) is 79% of that given by Equation (35) for a one stop trip with no return. Range as a function of ascent angle is shown for both the exact and approximate analyses in Figure XX. The large error obtained with this model reflects the pessimistic and dynamically incompatible descent phase.

## 7.0 SUMMARY

LFU multi-stop trajectory equations and computer programs for the impulsive, constant altitude-constant velocity, and semi-ballistic flight profiles have been developed. The resulting nonlinear equations require an iterative computation and are thus not suited to slide rule calculation.

A closed form approximate equation (27) for the constant velocity-constant altitude trajectory has been developed. This approximation shows good agreement with the exact equation for flight conditions of low velocity, low operational altitude and a few stops. A "rule of thumb" has been developed which shows the ratio of maximum impulsive trajectory range to maximum constant velocity-constant altitude trajectory range is 2:1.

The effect of flight variables including velocity, altitude, number of stops and payload on a baseline vehicle's range have been evaluated and are presented as curves. The conclusions from the analysis for the constant velocity-constant altitude trajectory are as follows:

- The range is greater when a payload is carried out with an empty return as compared with flying out empty and returning the same mass payload. The range difference increases with increasing payload, (Figure II). The range increase is approximately 7% for a 300 lb payload.
- Hover time over a point increases logarithmically with propellant loading for any vehicle. At zero altitude the hover time for the baseline vehicle is 11.9 min. Hover time is reduced 8.4% with operation at an altitude of 1500 ft, (Figures VI and VII).
- Total range is relatively insensitive to operational altitude for low velocities and a small number of stops. The range sensitivity increases with increasing horizontal velocity and/or an increasing number of stops, (Figures X and XVI).
- In a two segment trip with return to the point of departure, the propellant consumption for the out and return segments is independent of the trajectory altitude and velocity. This propellant division will be identical to that experienced by an impulsive vehicle with the same total velocity increment capability. For the baseline vehicle, 127 lb of the 230 lb total propellant weight are required for the out trip segment with no payload.

- At a given altitude and horizontal velocity, the decrease in range with an increasing number of stops is nearly linear and is less sensitive at lower velocities. If the baseline vehicle maintains a 50 ft altitude over a five stop sortie, the range increase with a 200 ft/sec velocity is 17.5% compared with a 250 ft/sec velocity (Figure XIII).
- At each ascent launch angle there is an optimum horizontal velocity and corresponding flight altitude which maximizes range. With increasing angles the altitude increases and the range increases to a maximum for a given velocity. An increase in the ascent angle also causes the optimum horizontal velocity to increase to a maximum value (Figure XII).
- Increasing the number of stops for a given vehicle significantly reduces the total range. The respective maximum baseline LFU ranges for two and six stops at a 50 ft altitude are 30.5 and 9.2 miles (Figure XIV). Carrying a 300 lb payload for the total distance reduces the maximum ranges to 14.9 and 4.3 miles for two and six stops.
- The optimum horizontal velocity at a given altitude decreases both with an increasing number of stops and increasing payload. For the baseline vehicle with no payload it is 463 and 147 ft/sec respectively for two and six stops, (Figure XV). The corresponding velocities when a 300 lb payload is carried are 324 and 100 ft/sec.
- A thrust/weight, (F/W), ratio of approximately two appears to be near the optimum relative to baseline LFU range capability and propulsion system throttling requirement (Figure XVII). If single engine operation of a dual engine system is not a mandatory safety requirement, the necessary propulsion throttling ratio is less than five with a F/W ratio of two.

With a semi-ballistic trajectory, a greater percentage range loss is experienced with an increasing number of stops. For the baseline LFU this loss is 50% for a two stop sortie as compared with a one stop trip. Maximum range for this trajectory is 88% of optimum constant velocity-constant altitude trajectory range for a single stop round trip.

The semi-ballistic trajectory requires more complex guidance and control equipment than the constant velocity-constant elevation trajectory and is thus less suited to a

minimal LFU development and qualification program. For long trip segments the high velocities and high maximum ordinates present significant astronaut hazards in the event of an in-flight malfunction. After a particular trajectory segment flight has been initiated, an in-flight range reduction is not possible without waste of vehicle velocity increment capability.

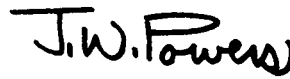
The analysis does not consider any inability of the astronaut/vehicle system to maintain constant attitude during ascent and descent or constant altitude during horizontal flight. Hovering during landing or take-off and landing at non-optimum (less than maximum) thrust were not considered. The sum of these factors could significantly reduce the range as predicted by the developed equations.

The baseline vehicle's weight estimates are optimistic. A current prediction for the structural and propulsion inert weight is 190 lb rather than 150 lb. A suited astronaut's weight including a portable life support system is currently estimated at 370 lb rather than 300 lb. To obtain the performance indicated for the lighter baseline vehicle with current weight estimates, approximately 290 lb of propellant rather than 230 lb will have to be provided.

A linearized range approximation for the constant velocity-constant altitude trajectory with many stops has been developed (Appendix I).

## 8.0 ACKNOWLEDGMENT

Miss Carol Banick and Miss Judith Bartleson assiduously programmed the majority of the equations used in the data presentation. Mr. P. H. Whipple thoroughly reviewed most of the analysis and found several errors. His constructive criticism in several other areas is also appreciated. Mr. C. O. Guffee gave valuable programming advice and programmed several of the equations. Miss Maryetta Fine incorporated the many draft revisions both accurately and cheerfully.

  
J. W. Powers

1022-JWP-mef

Attachments  
Appendix I  
Figures I - XX  
References

# BELLCOMM, INC.

## APPENDIX I

### CONSTANT ALTITUDE - CONSTANT VELOCITY TRAJECTORY, LINEARIZED ANALYSIS

For a many stop sortie, the amount of propellant expended in a trip segment will be small compared with the total vehicle mass at the initiation of thrusting. This situation allows the expressions  $\ln (1 - \dot{m}t/M)$  to be approximated by the first term of the series expansion. Using this technique the equations of Section 5.0 may be significantly simplified.

By use of (19), trajectory altitude is

$$H = \frac{1}{2g} \left( \frac{C \sin \phi \dot{m} t_A}{M_{oi}} \right)^2$$

By use of (20), powered descent time is

$$t_D = \frac{t_A M_{fi} \cos \phi}{M_{oi} \cos \theta}$$

By use of (24), coast ascent time is

$$t_{cA} = t_A \left( \frac{C \sin \phi \dot{m}}{g M_{oi}} - 1 \right)$$

By use of (21.1), coast descent time is

$$t_{cD} = t_D \left( \frac{C \sin \theta \dot{m}}{g M_{fi}} - 1 \right)$$

If the amount of propellant expended in the  $i^{\text{th}}$  segment of  $N$  stop sortie is  $M_{pi}$ , hover time may be determined from (17). For a many stop sortie the denominator term  $m \dot{t}_A$  may be ignored in comparison with  $M_{oi}$ . Hover time may thus be written

$$t_H = \frac{C}{g} \left[ \frac{M_{pi} - m \dot{t}_A (t_A + t_D)}{M_{oi}} \right]$$

where  $M_{oi} = M_{pi} + M_{fi}$  and

$$M_p = \sum_{i=1}^N M_{pi}$$

$$M_{oi} = M_o - \sum_{i=1}^{i-1} M_{pi}$$

Total flight time at the constant horizontal velocity,  $V_x$ , is  $(t_{cA} + t_H + t_{cD})$ . If the horizontal velocity is assumed to be developed by a constant acceleration, the horizontal distances traveled during the acceleration and retro phases are  $V_x t_A/2$  and  $V_x t_D/2$  where

$$V_x = C \cos \phi \dot{m} t_A / M_{oi}$$

The range segment  $R_1$  is

$$R_1 = V_x (t_A/2 + t_{cA} + t_H + t_{cD} + t_D/2)$$



After substitution of previously developed terms, algebraic simplification and use of the assumption  $\theta = \phi$ .\*

$$R_1 = \frac{\dot{m} \cos \phi}{g} \left( \frac{C}{M_{oi}} \right)^2 t_A \left\{ t_A \left[ 2 \sin \phi \dot{m} - \left( 1 + \frac{M_{fi}}{M_{oi}} \right) \left( \dot{m} + \frac{g M_{oi}}{2 C} \right) \right] + M_{pi} \right\}$$

The ascent time for maximum range is

$$(t_A)_{opt} = \frac{M_{pi}}{2 \dot{m} \left[ \left( 1 + \frac{M_{fi}}{M_{oi}} \right) \left( 1 + \frac{g M_{oi}}{2 \dot{m} C} \right) - 2 \sin \phi \right]}$$

The corresponding optimum flight altitude for maximum range can be determined from the above equation and the first equation listed in this appendix.

Summation of all the range segments yields the total traveled distance.

$$R = \sum_{1}^N R_1$$

Comparison with the numerical results of Section 5.0 shows a range error of approximately -9.5% for the baseline LFU on a round trip ( $\phi=30^\circ$  and  $V_x=100$  ft/sec). This error will significantly decrease with an increasing number of stops. The corresponding error in optimum powered ascent time for maximum range is about 5%.

---

\*Numerical calculations from Section 5.0 show the maximum angular difference ( $\phi-\theta$ ) to be  $<4.5^\circ$  for a round trip. With an increasing number of stops, this angular difference decreases.

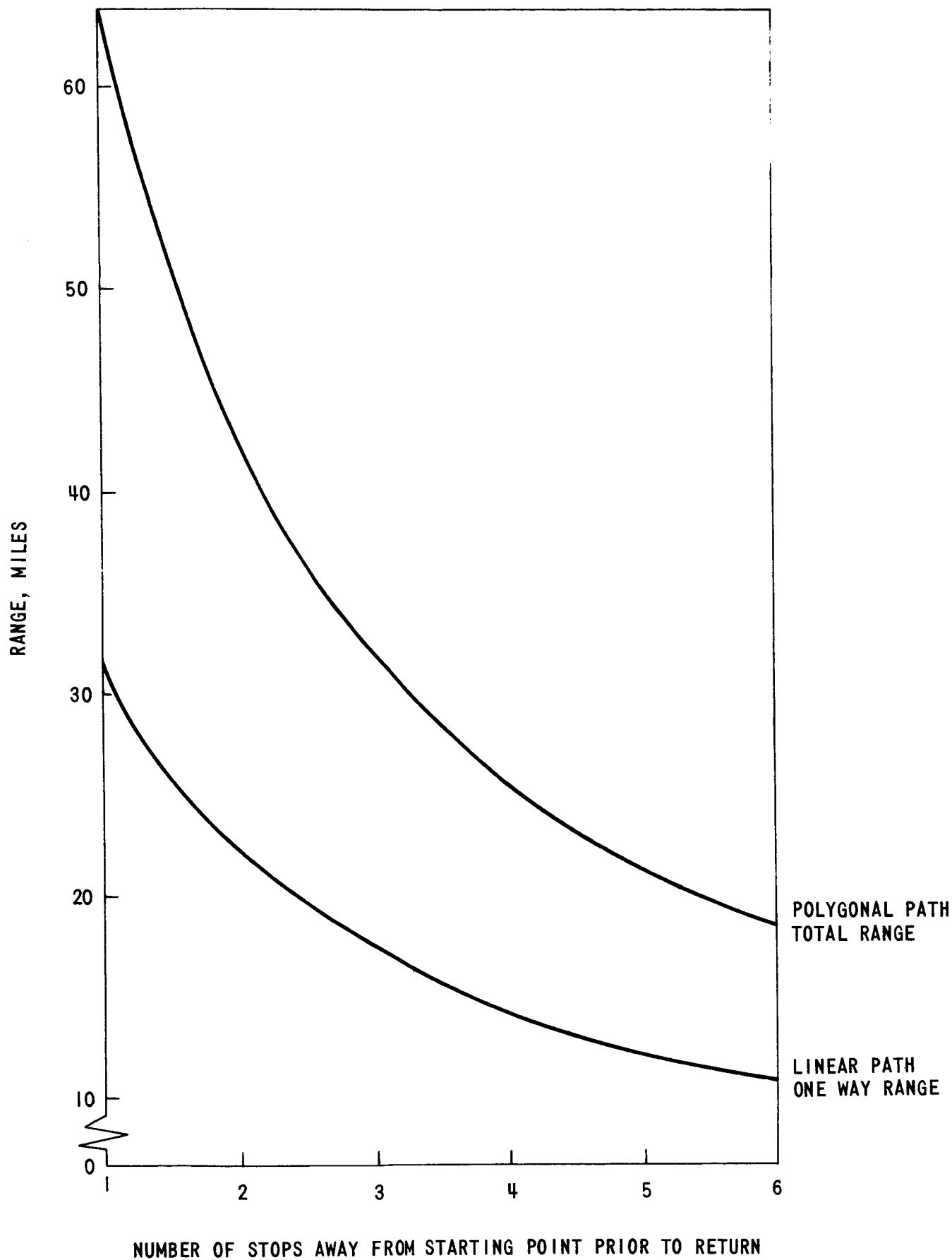


FIGURE 1 - BASELINE LFU RANGE vs. NUMBER OF EQUAL LENGTH STOPS, IMPULSIVE VELOCITY INCREMENTS

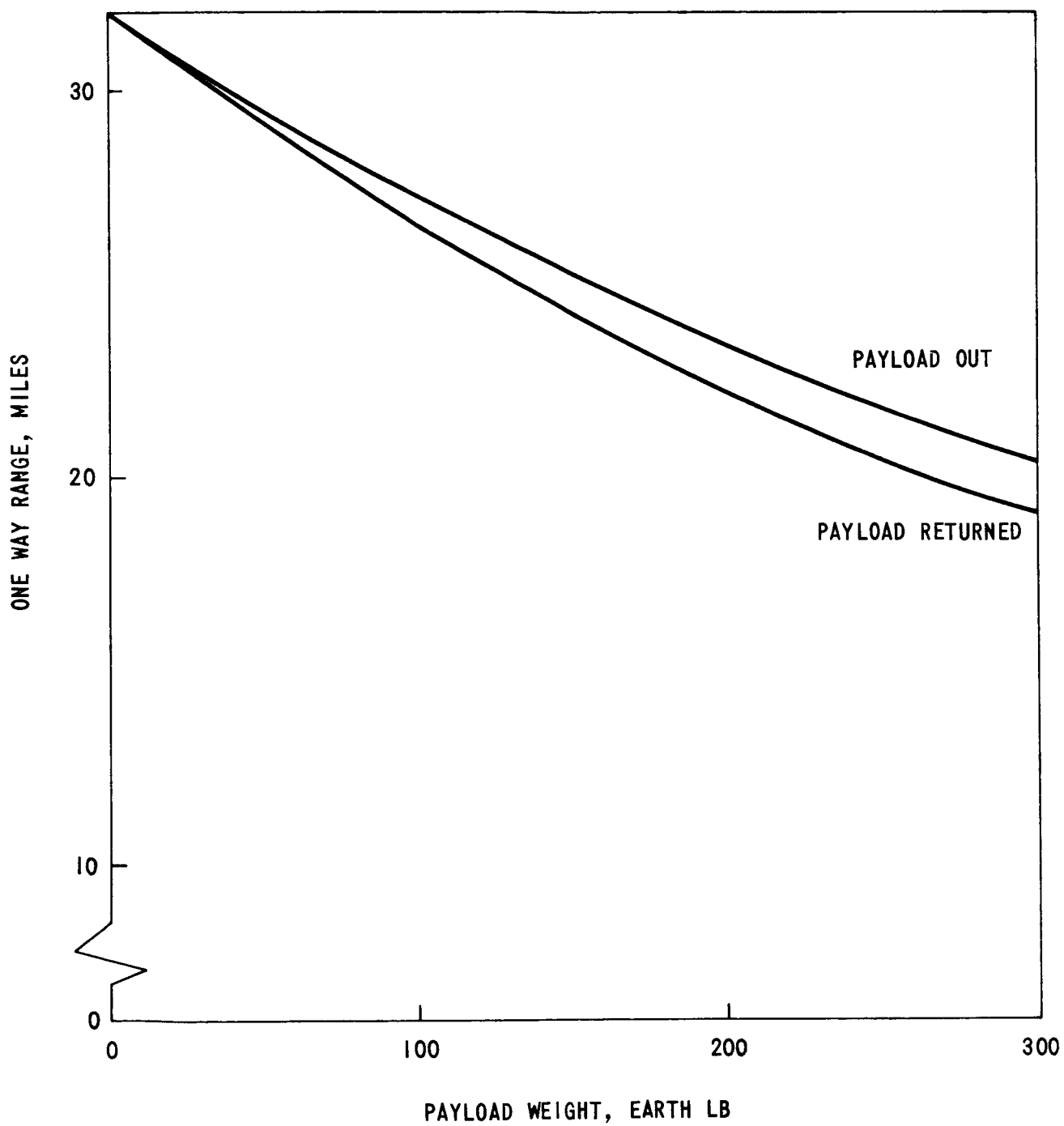


FIGURE 11 - BASELINE LFU RANGE vs. PAYLOAD RETURNED OR DELIVERED,  
SINGLE STOP, IMPULSIVE VELOCITY INCREMENTS

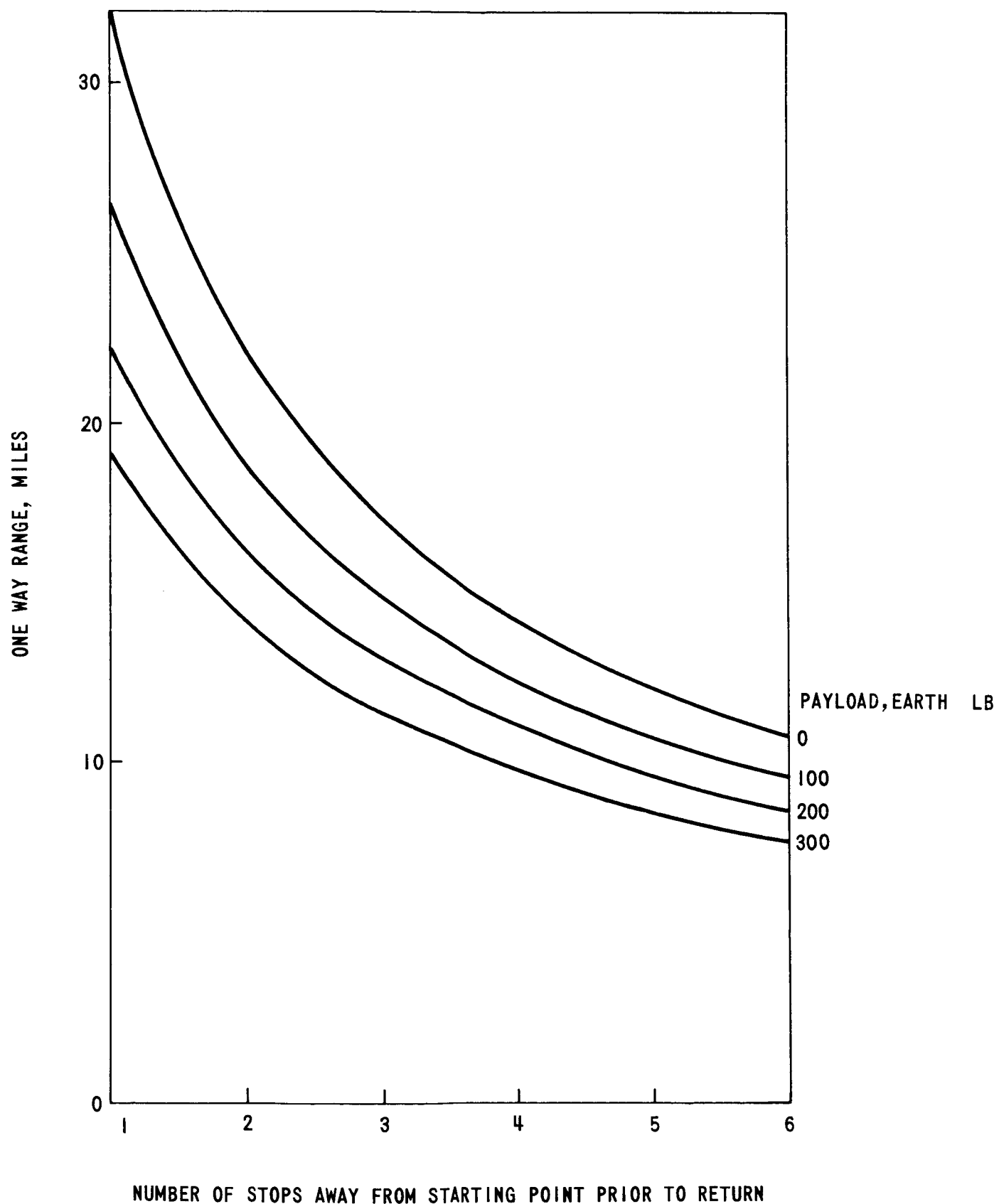


FIGURE III - BASELINE LFU LINEAR RANGE vs. NUMBER OF STOPS, PAYLOAD FROM LAST STOP PRIOR TO RETURN, IMPULSIVE VELOCITY INCREMENTS, EQUAL LENGTH SEGMENTS

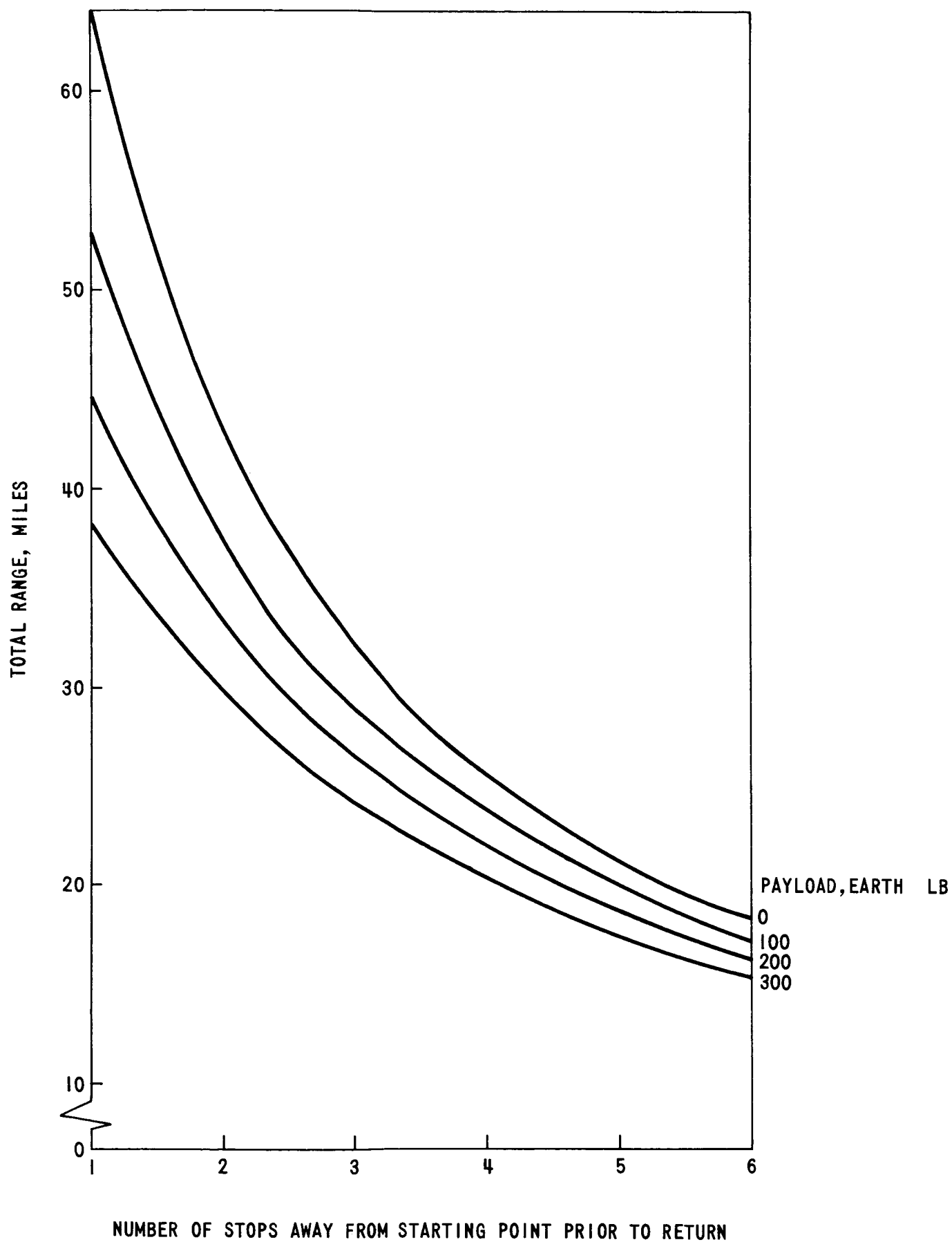


FIGURE IV - BASELINE LFU TOTAL POLYGON RANGE vs. NUMBER OF STOPS, PAYLOAD FROM LAST STOP PRIOR TO RETURN, IMPULSIVE VELOCITY INCREMENTS, EQUAL LENGTH SEGMENTS

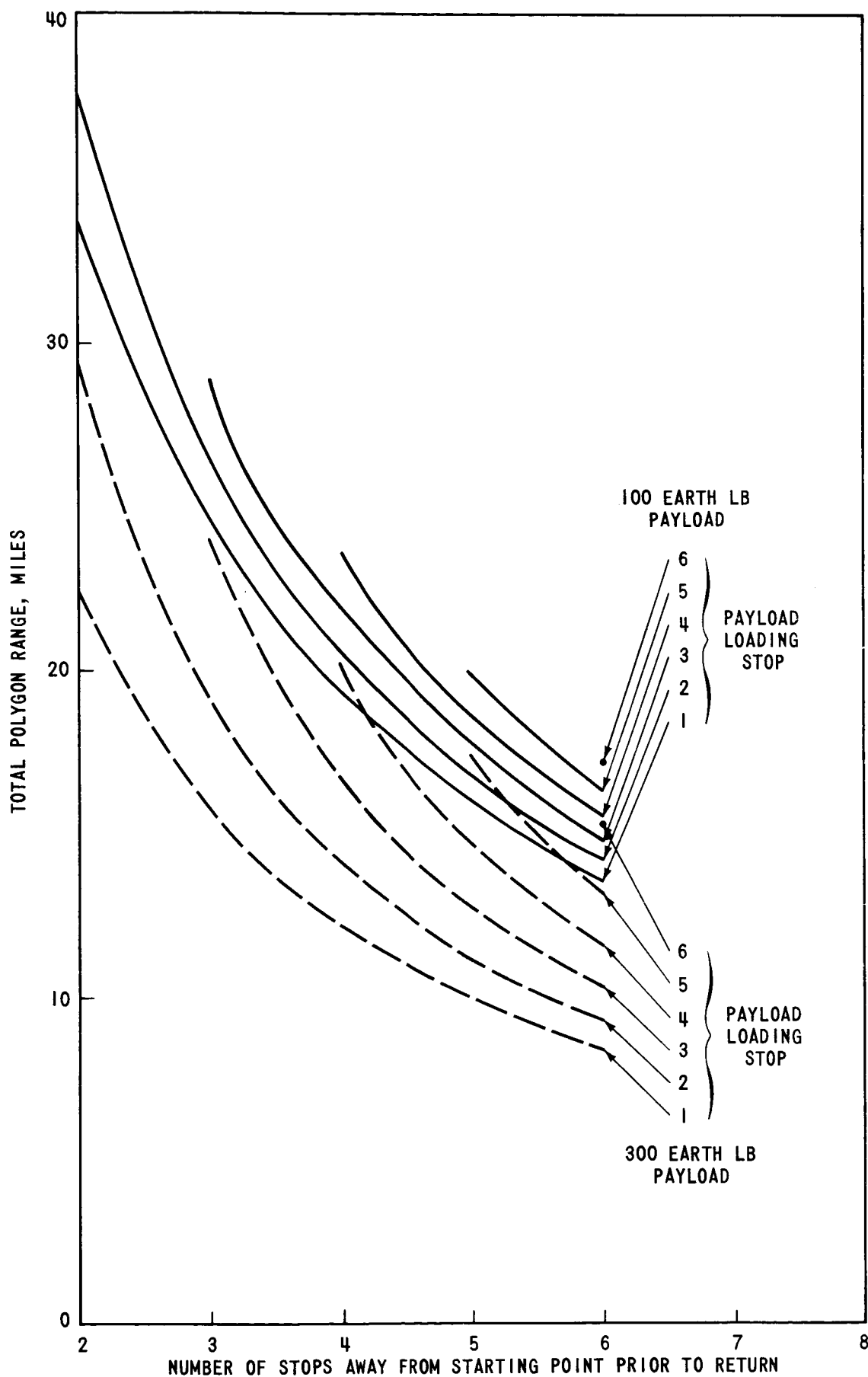


FIGURE V - BASELINE LFU TOTAL POLYGON RANGE vs. NUMBER OF STOPS FOR DIFFERENT PAYLOADS AND LOADING STOPS, IMPULSIVE VELOCITY INCREMENTS, EQUAL LENGTH STOPS

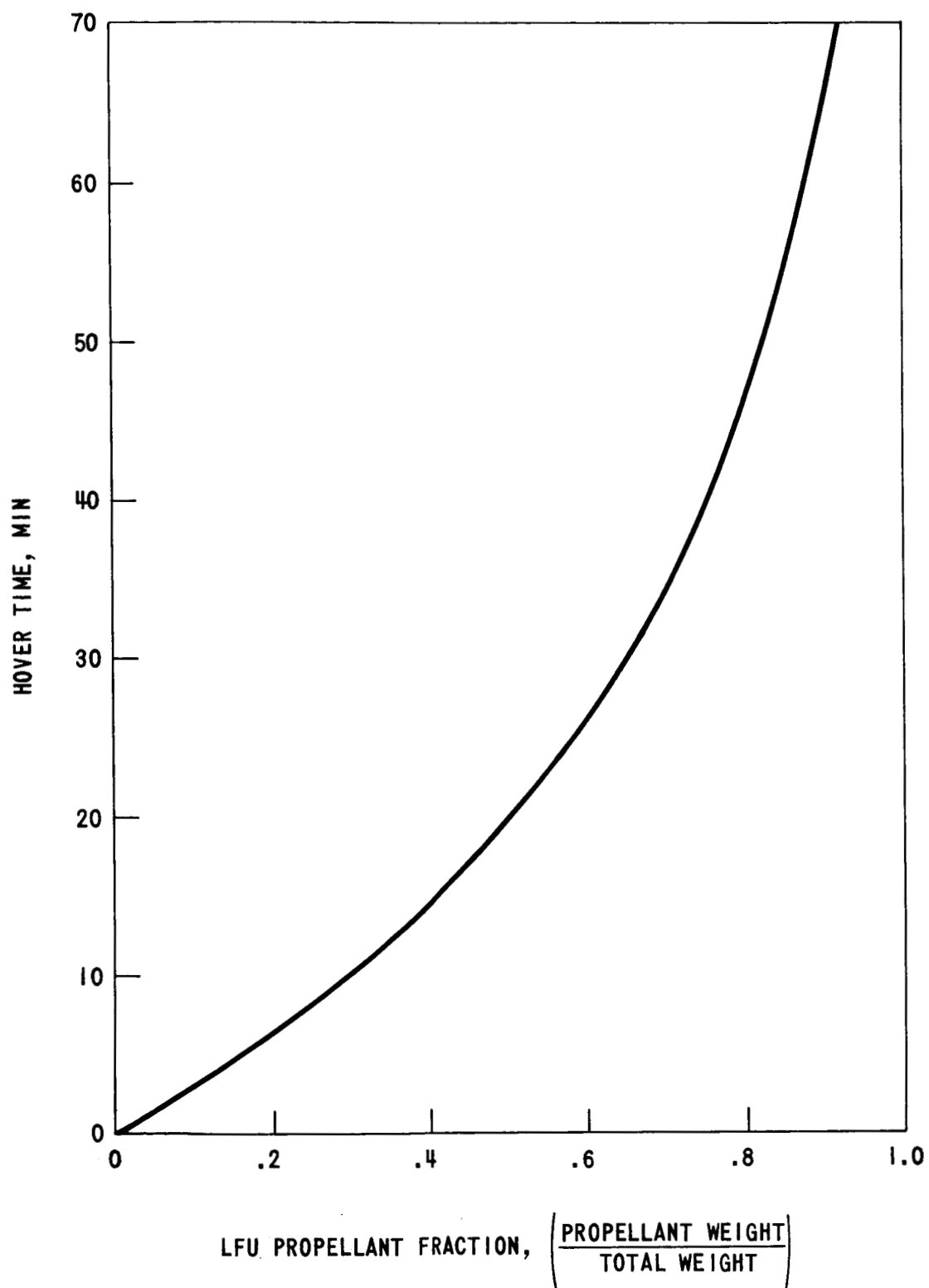


FIGURE VI - HOVER FLIGHT TIME vs. LFU PROPELLANT FRACTION, ZERO ALTITUDE OVER A GIVEN POINT

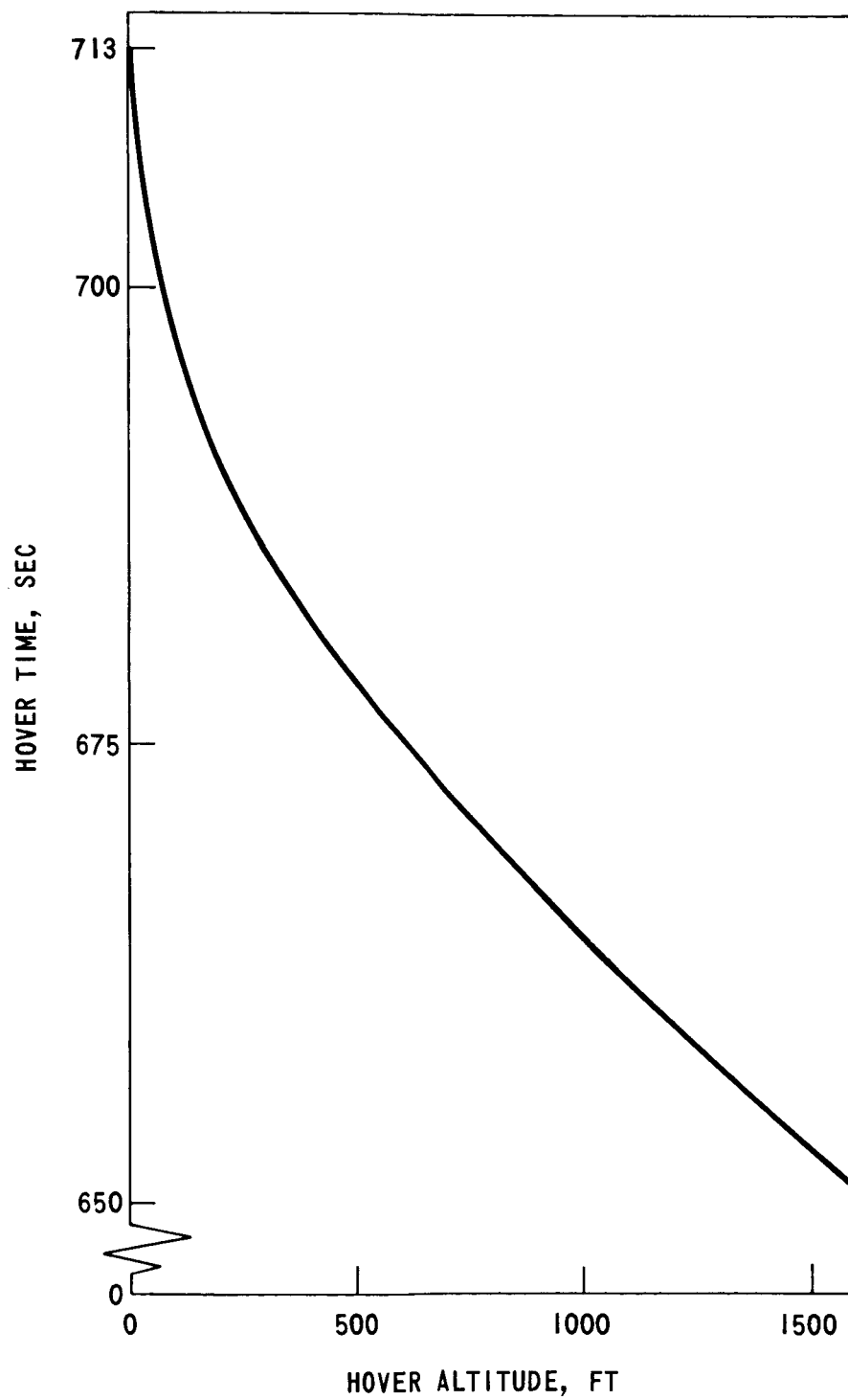


FIGURE VII - BASELINE LFU HOVER FLIGHT TIME OVER A GIVEN POINT, vs. HOVER ALTITUDE



# TRAJECTORY PHASES

- AB: POWERED CONSTANT ALTITUDE - CONSTANT THRUST ASCENT
- BC: UNPOWERED COAST ASCENT
- CD: CONSTANT ALTITUDE - CONSTANT VELOCITY (THRUST= WEIGHT)
- DE: UNPOWERED COAST DESCENT
- EF: POWERED CONSTANT ALTITUDE - CONSTANT THRUST DESCENT

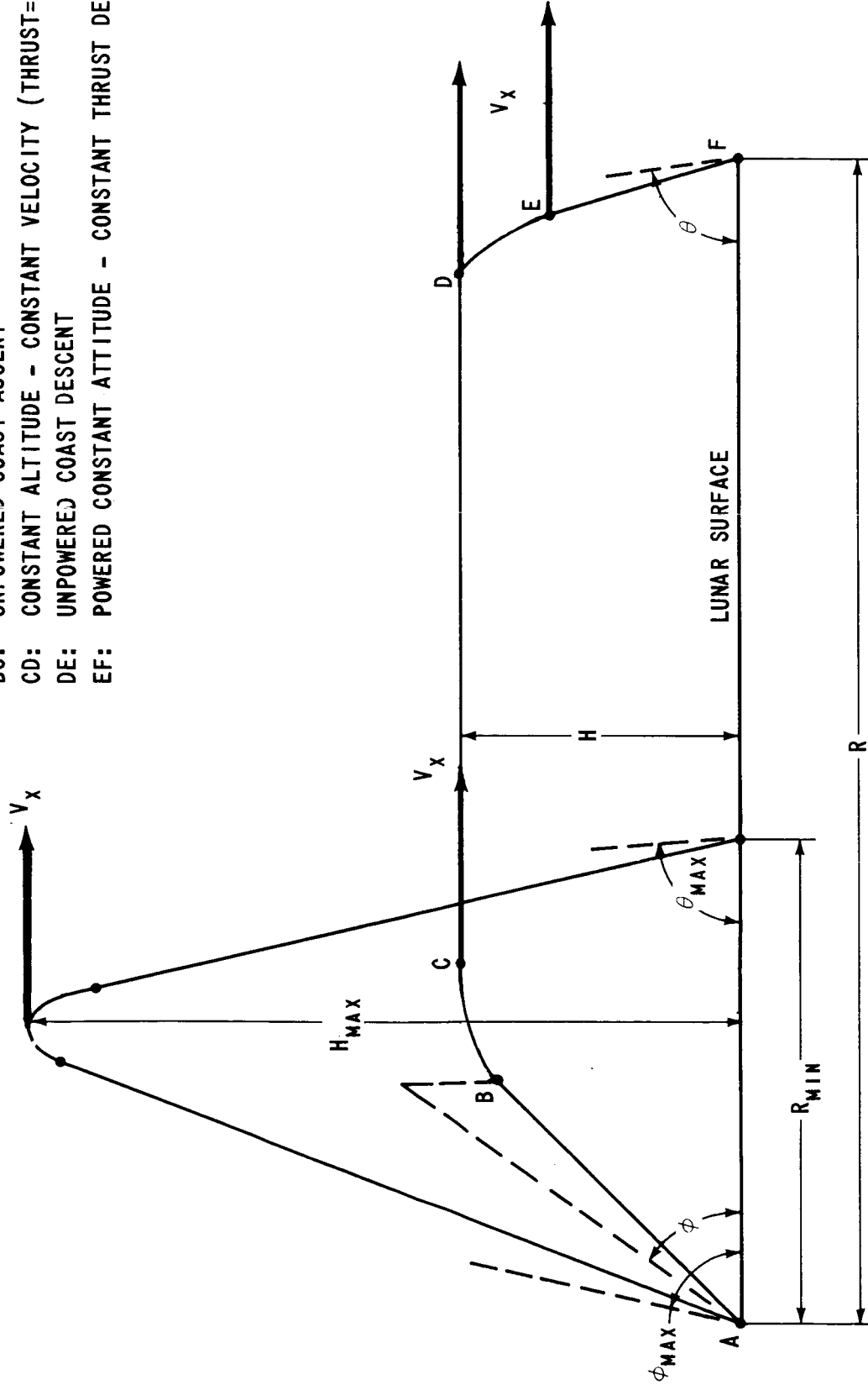


FIGURE VIII - LFO CONSTANT HORIZONTAL VELOCITY TRAJECTORY PROFILES

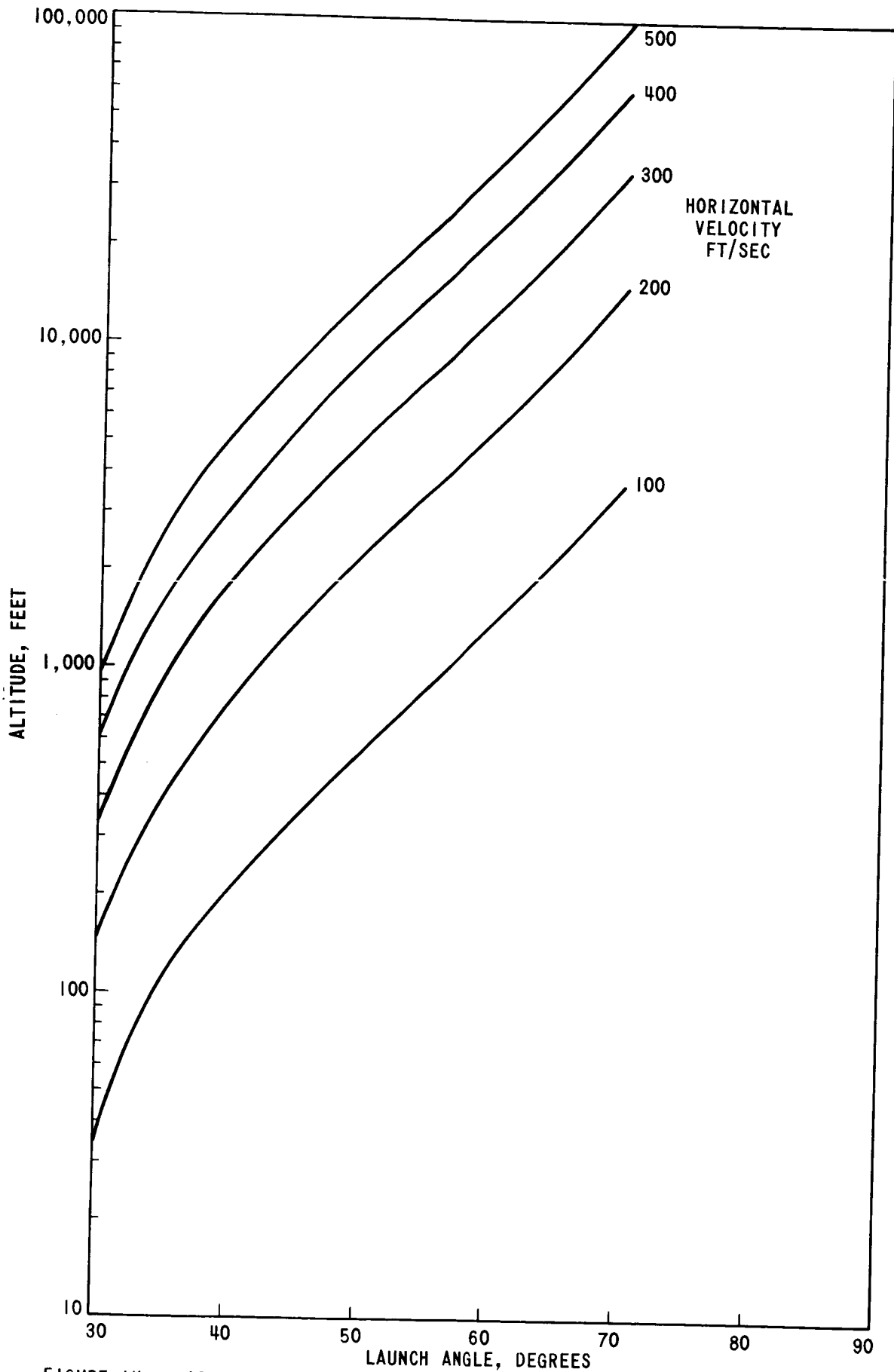


FIGURE IX - BASELINE LFU CONSTANT ALTITUDE TRAJECTORY, ALTITUDE vs. LAUNCH ANGLE AS A FUNCTION OF HORIZONTAL VELOCITY

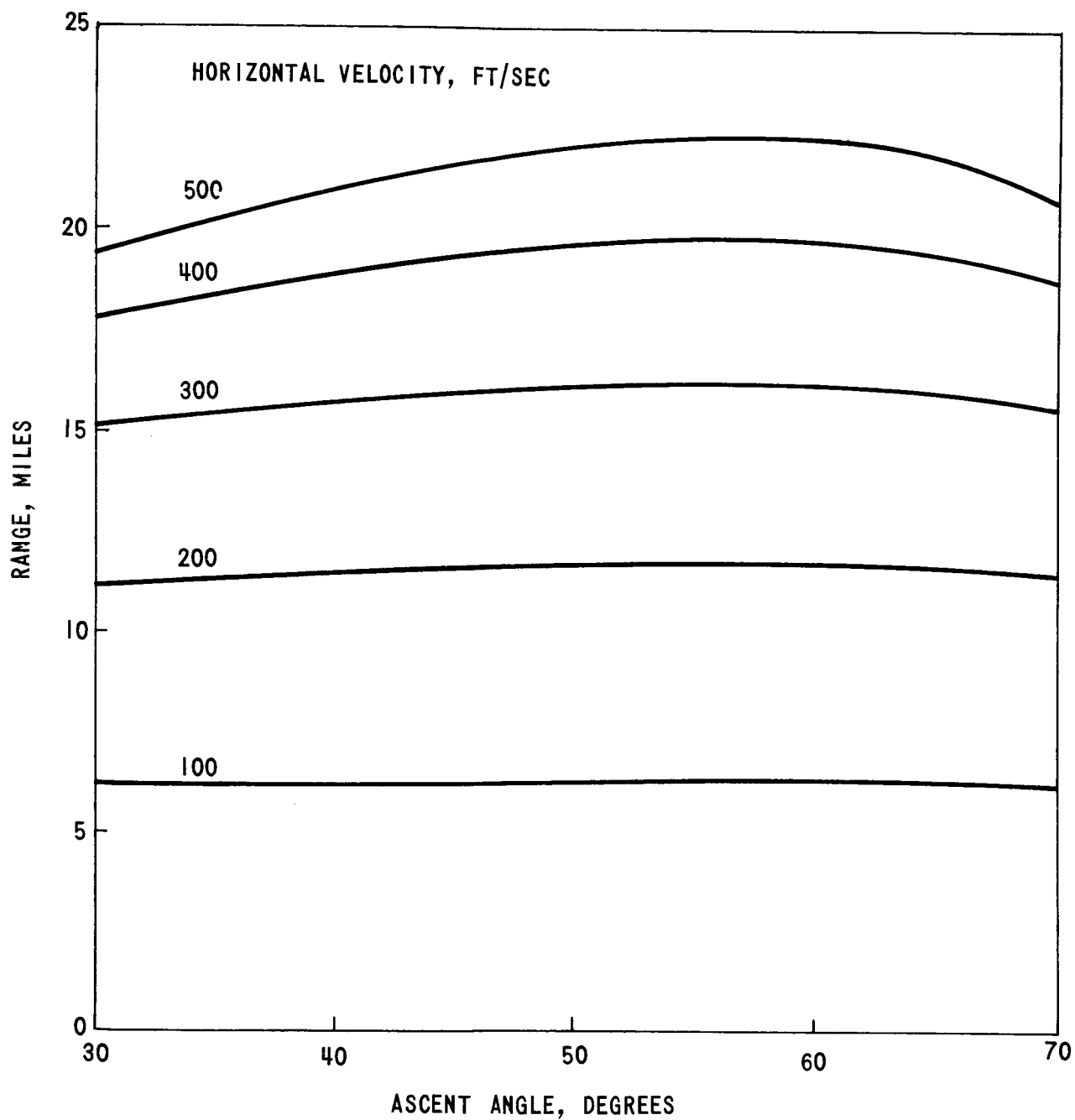


FIGURE X - BASELINE LFU CONSTANT ALTITUDE TRAJECTORY, RANGE vs. ASCENT ANGLE AS A FUNCTION OF HORIZONTAL VELOCITY

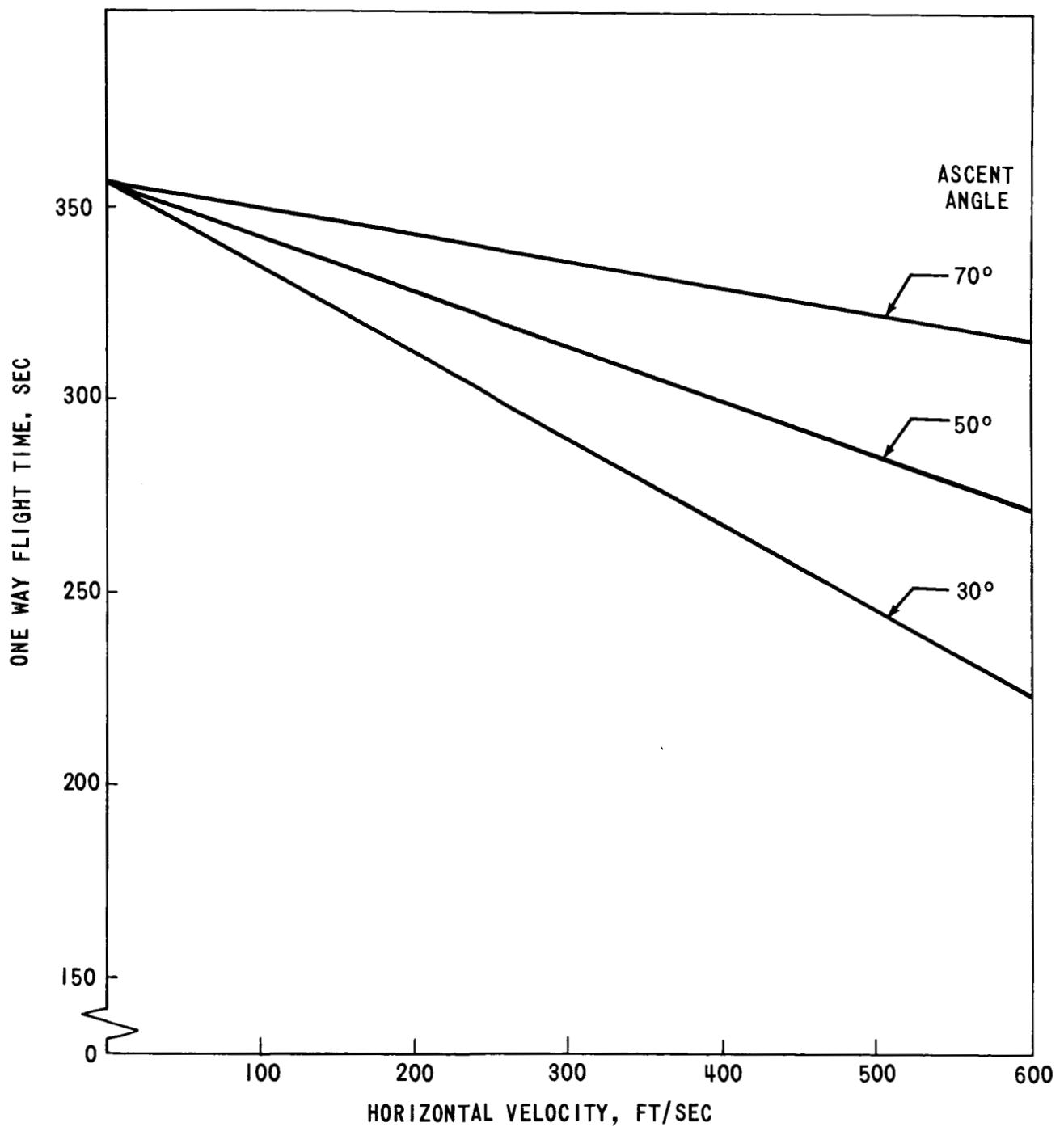


FIGURE XI - BASELINE LFU CONSTANT ALTITUDE TRAJECTORY ONE WAY FLIGHT TIME OF ROUND TRIP SORTIE vs. HORIZONTAL VELOCITY AS A FUNCTION OF ASCENT ANGLE

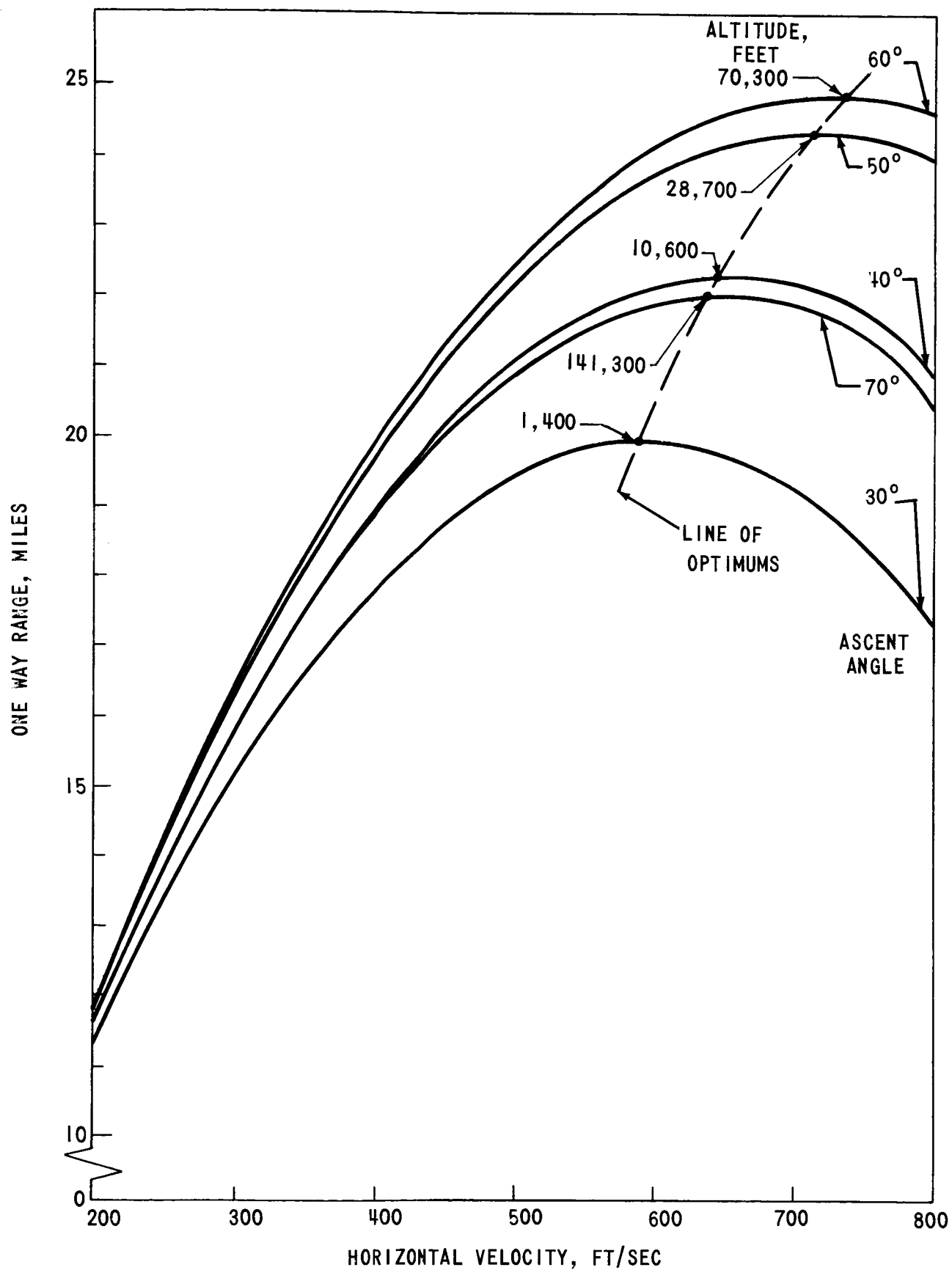


FIGURE XII - BASELINE LFU CONSTANT ALTITUDE TRAJECTORY, ONE WAY RANGE vs. HORIZONTAL VELOCITY AS A FUNCTION OF ASCENT ANGLE (ALTITUDE)

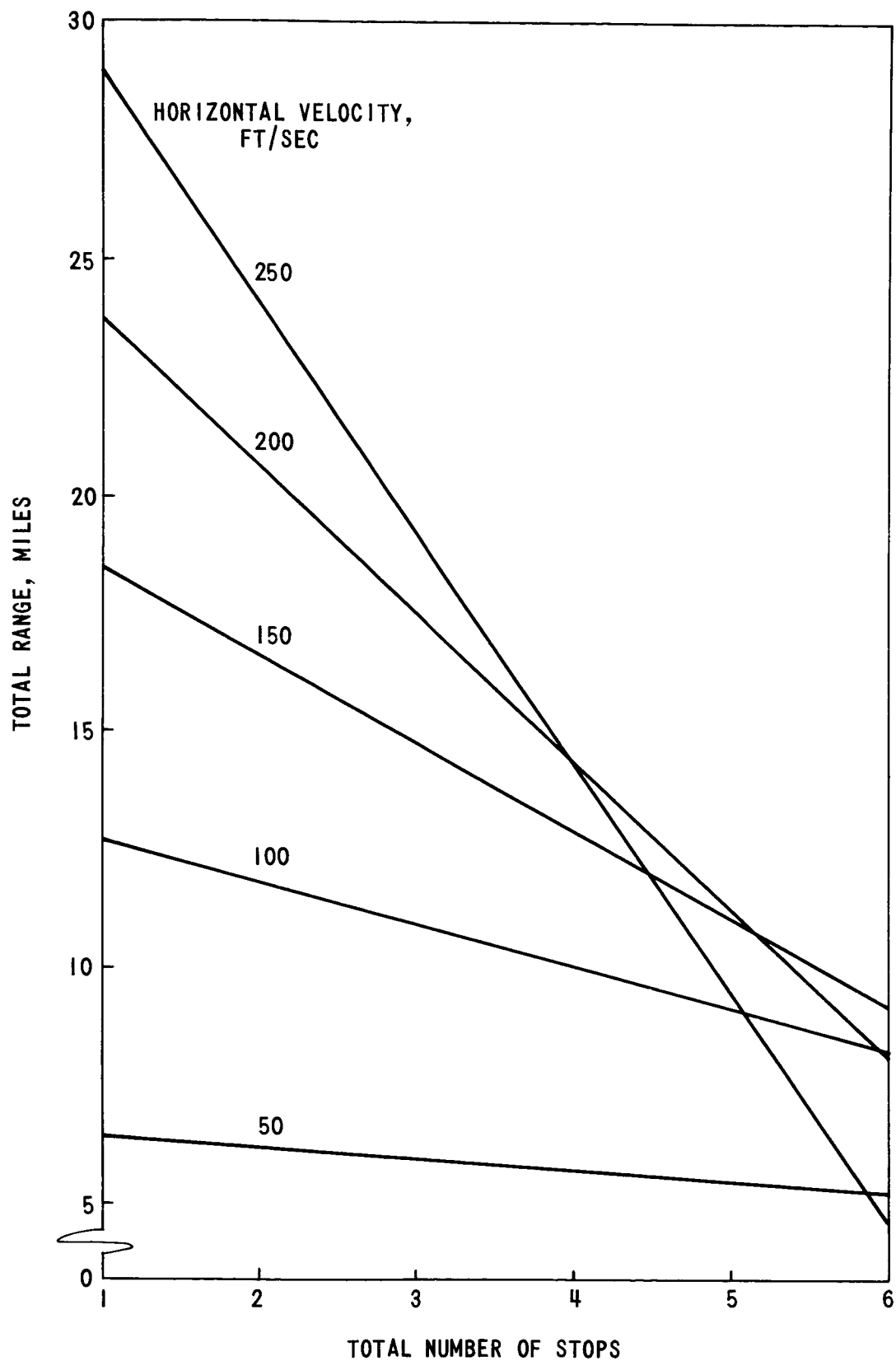


FIGURE XIII - BASELINE LFU TOTAL RANGE vs. TOTAL NUMBER OF STOPS AS A FUNCTION OF HORIZONTAL VELOCITY - CONSTANT ALTITUDE (50') TRAJECTORY

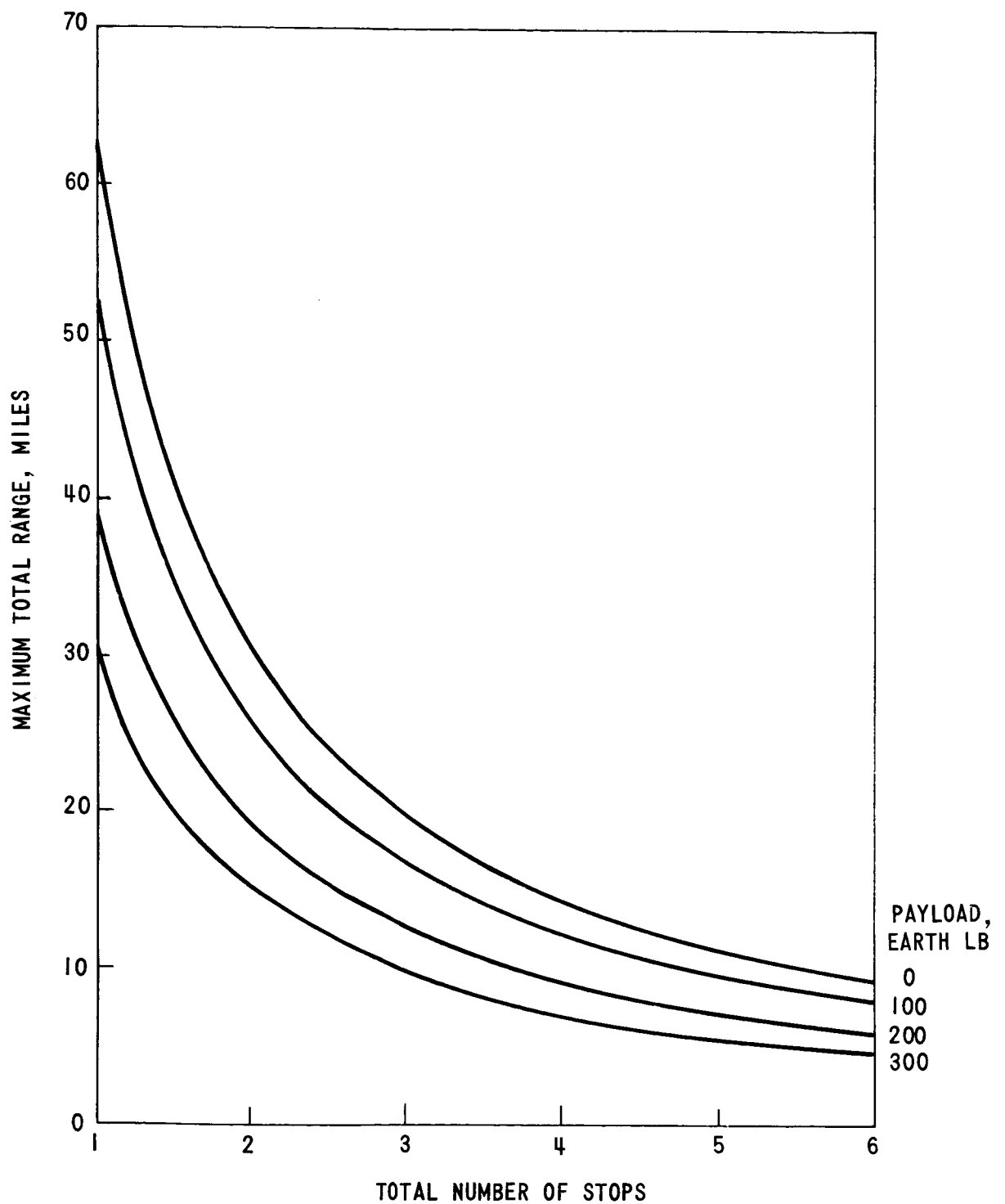


FIGURE XIV - BASELINE LFU MAXIMUM TOTAL RANGE vs. TOTAL NUMBER OF STOPS FOR DIFFERENT PAYLOADS, CONSTANT VELOCITY - CONSTANT ALTITUDE (50') TRAJECTORY

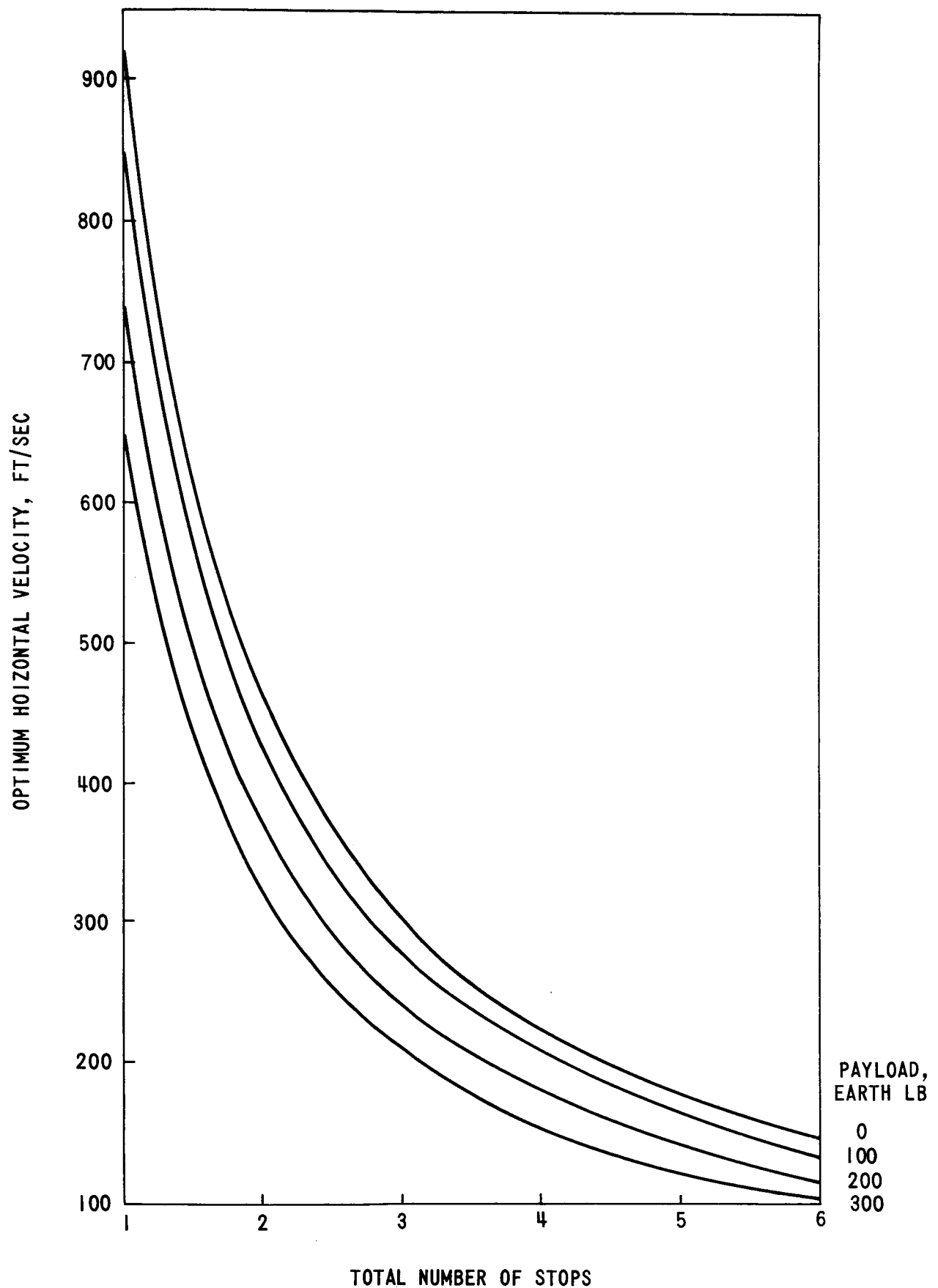


FIGURE XV - BASELINE LFU OPTIMUM HORIZONTAL VELOCITY vs. TOTAL NUMBER OF STOPS FOR DIFFERENT PAYLOADS, CONSTANT VELOCITY - CONSTANT ALTITUDE (50') TRAJECTORY



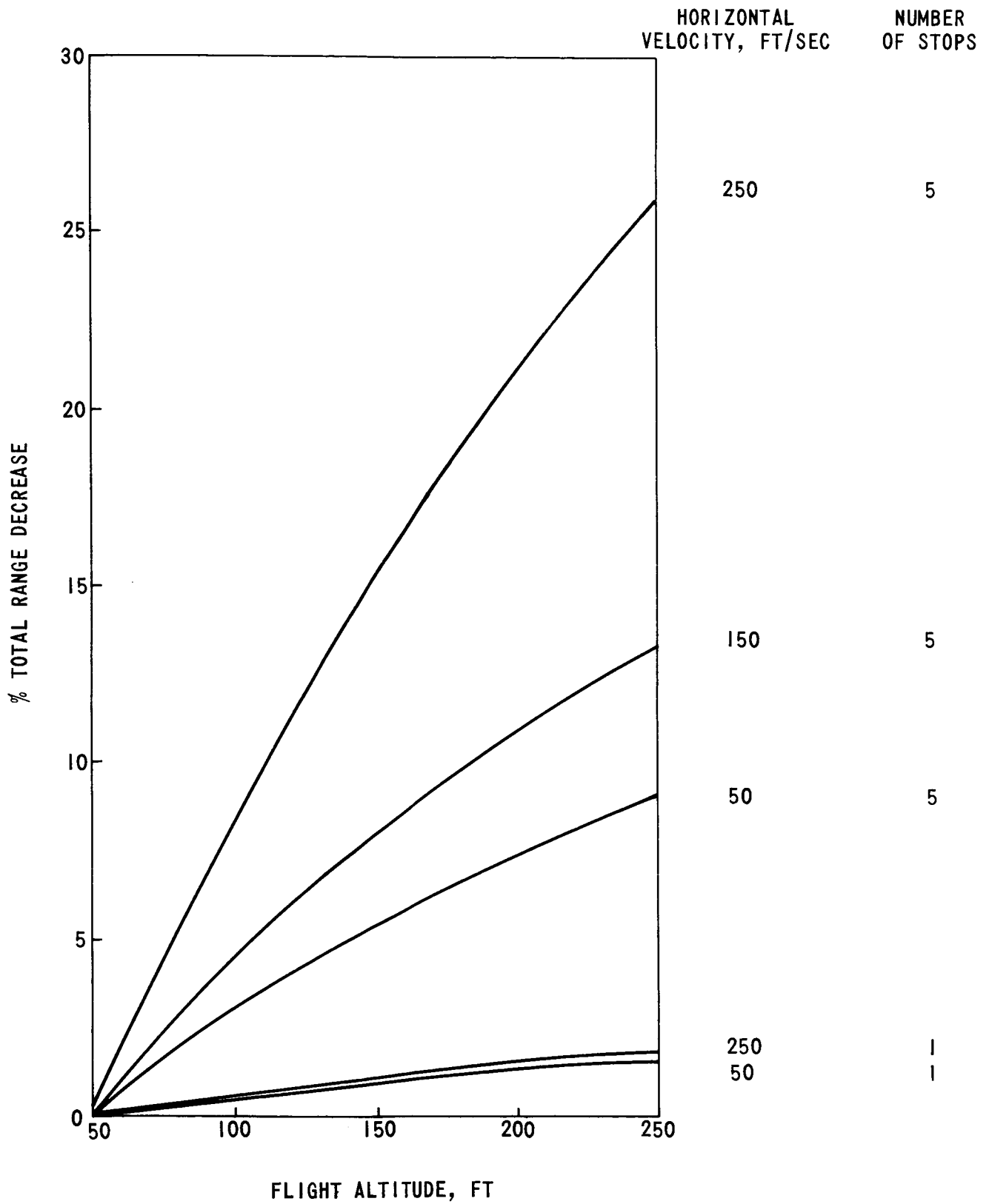


FIGURE XVI - BASELINE LFU % RANGE DECREASE vs. FLIGHT ALTITUDE  
AS A FUNCTION OF HORIZONTAL VELOCITY & NUMBER OF STOPS

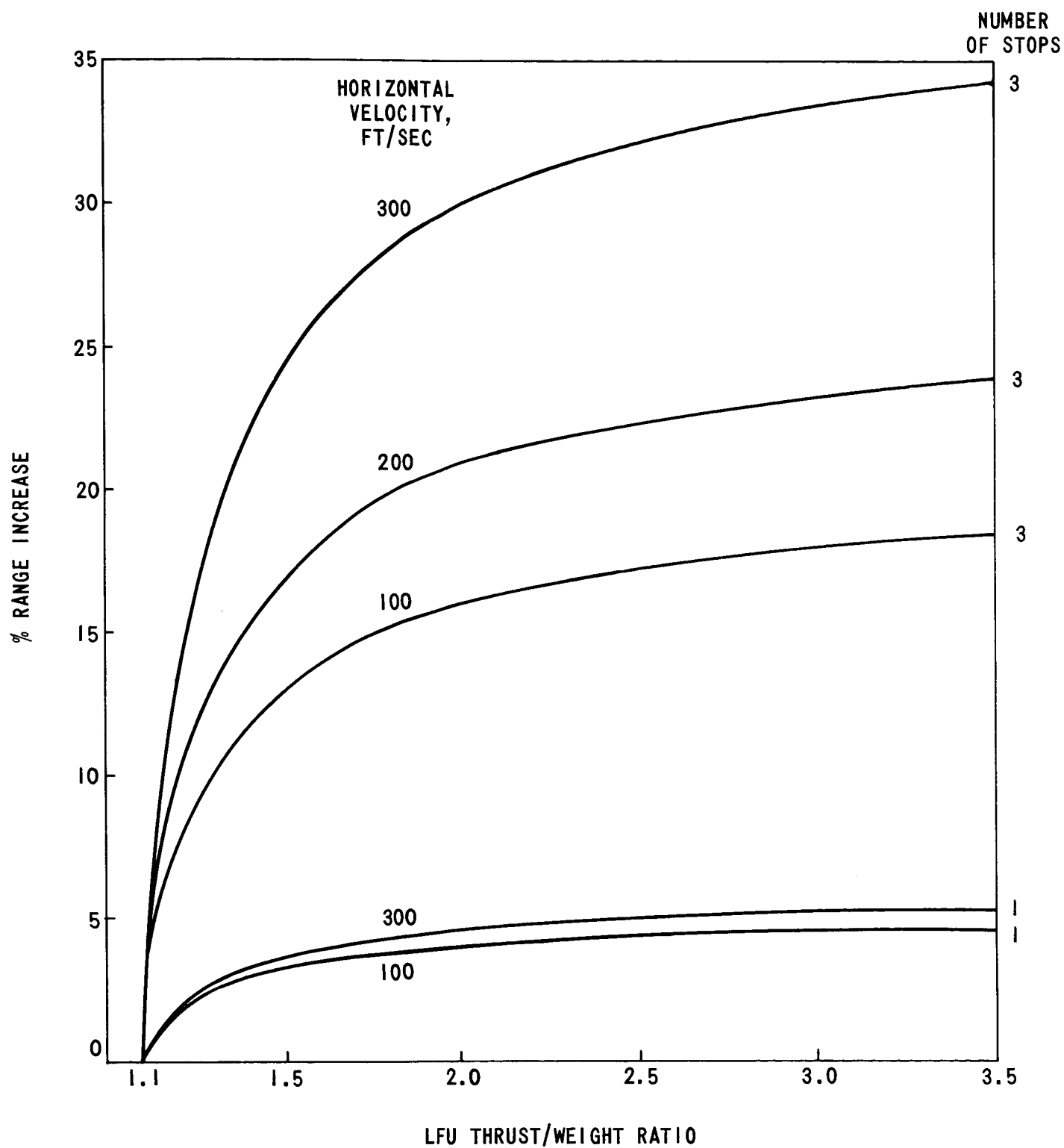


FIGURE XVII - BASELINE LFU % RANGE INCREASE vs. THRUST/WEIGHT RATIO  
FOR DIFFERENT HORIZONTAL VELOCITIES & NUMBER OF STOPS.  
100 FT ALTITUDE

# TRAJECTORY PHASES

- AB: POWERED CONSTANT ATTITUDE - CONSTANT THRUST ASCENT
- BC: POWERED COAST (THRUST VECTOR DECREASED & DIRECTED UPWARD)
- CD: POWERED CONSTANT ATTITUDE - CONSTANT THRUST DESCENT

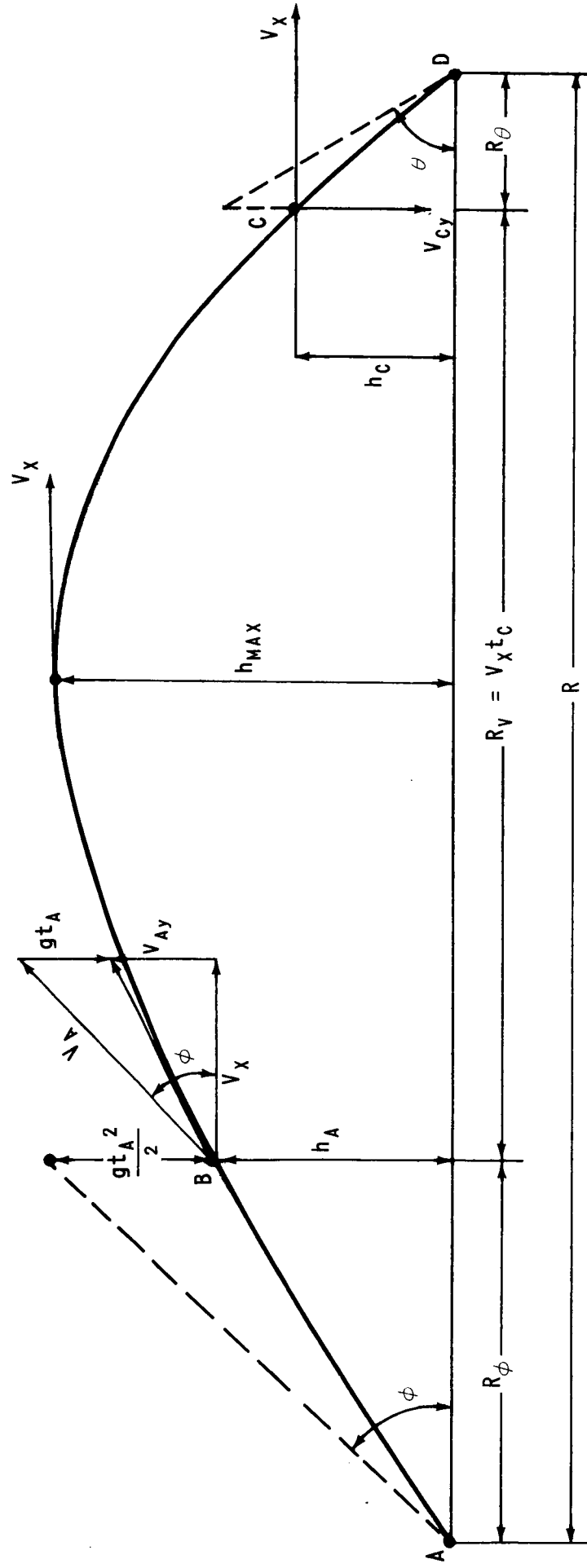


FIGURE XVIII - LFU SEMI-BALLISTIC TRAJECTORY

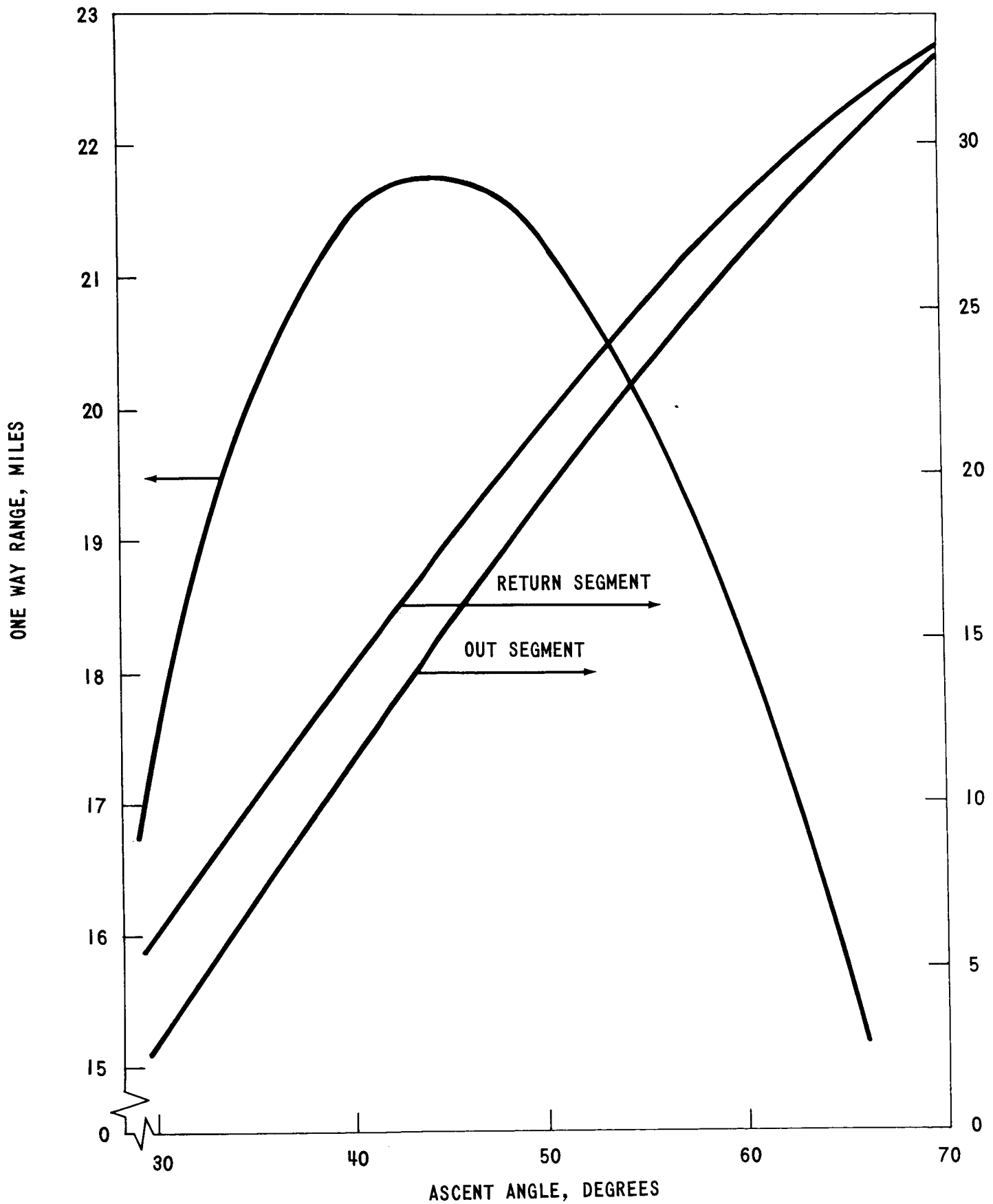


FIGURE XIX - BASELINE LFU ONE WAY RANGE & MAXIMUM TRAJECTORY ALTITUDE vs. ASCENT ANGLE, SEMI-BALLISTIC TRAJECTORY

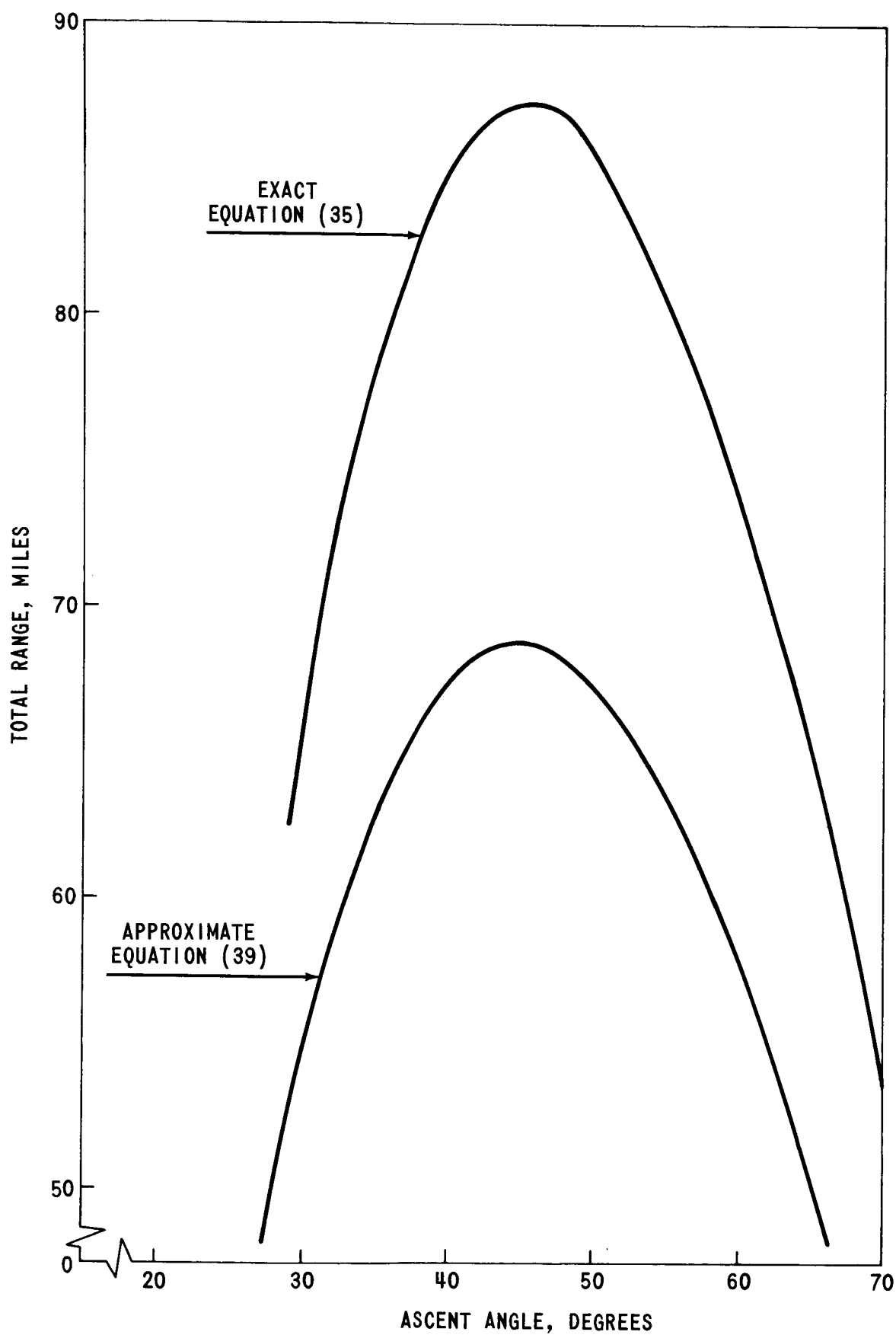


FIGURE XX - BASELINE LFU TOTAL RANGE (NO RETURN) vs. ASCENT ANGLE, SEMI-BALLISTIC TRAJECTORY

BELLCOMM, INC.

REFERENCES

1. "Study of Manned Flying Systems", (Summary) Report 7243-950003, Bell Aerosystems, June 1966, p. 11.
2. Principles of Guided Missile Design: Aerodynamics, Propulsion, Structures and Design Practice, Bonney, Zucrow, and Besserer  
D. VanNostrand, p. 382, Equation 8-82.